Intrinsic correlation between superconductivity and magnetism

Xiuqing Huang*
[1]*Department of Telecommunications Engineering ICE, Army Engineering University, Nanjing 210007, China*
[2]*Department of Physics and National Laboratory of Solid State Microstructure, Nanjing University, Nanjing 210093, China*
(Dated: April 7, 2023)

Based on the real-space Mott insulator model, we have found a unified pairing, coherent and condensate mechanism of superconductivity for all materials. Partly motivated by Dirac's magnetic monopole and Maxwell's displacement current hypothesis, we demonstrate that electric and magnetic fields are intrinsically relevant. An isolated proton or electron creates an electric field, whereas a real-space quantized proton-electron pair creates a magnetic field. These findings offer new insights into the nature of electron spin, magnetic monopoles, and the symmetry of Maxwell's equations. We argue that the electric dipole vector of the proton-electron pair plays the role of the Ginzburg-Landau order parameter in the superconducting phase transition. It appears that the Peierls transition of the electron-proton electric dipole lattice leads to the symmetry breaking of the Mott insulating state and the emergence of superconducting and magnetic states. With this theoretical framework, the Meissner effect, London penetration depth, magic doping, flux neutralization, vortex lattice, and vortex dynamics, among other superconducting phenomena, can be comprehensively explained.

PACS numbers: 71.10. w, 74.20. z, 74.25.Ha, 75.10.–b

I. INTRODUCTION

Since Kamerlingh Onnes discovered superconductivity in mercury [1], thousands of superconducting elements and compounds have been found [2–11]. From a fundamental physics point of view, these superconducting materials can be classified into two categories: conventional and unconventional. It is widely accepted that BCS electron-phonon theory [12] can well describe conventional superconductors, while unconventional superconductors cannot be successfully explained by BCS theory. The research explosion in superconductivity began with Bednorz-Muller's groundbreaking discovery [4]. Following Cooper's pairing model, physicists have spent 37 years investigating the mechanism of high-temperature superconductivity (pairing glue). Despite publishing more than 200,000 studies, proposing hundreds of microscopic theories to unravel the mystery based on the rich phase diagram (see Fig. 1) [13–22], none have been deemed valid [23]. In response to this, Anderson publically challenged the existence of pairing glue responsible for pairing electrons in cuprate superconductors [24].

It is unconventional that despite extensive and intensive research efforts, superconductivity remains poorly understood. The physics community must now seriously question whether some fundamental blunders have led us astray. Perhaps some commonly accepted theories or models fail to capture the essence of the superconducting phenomenon [25, 26]. In my opinion, the problem of understanding high-temperature superconductivity is a new dark cloud looming over the field of physics. To solve this puzzle, we must break free from our old theoretical framework which has confined our thinking until now. Undeniably, high-temperature superconductivity is achieved through doping, which means that high-temperature superconductors are highly disordered materials. Consequently, the electronic energy-band theory based on perfect crystals is unsuitable for studying strongly correlated superconducting systems. Furthermore, researchers should no longer waste time and effort getting entangled in the so-called pairing glue, as suggested by Anderson. Instead, they must focus their efforts on considering the following crucial questions.

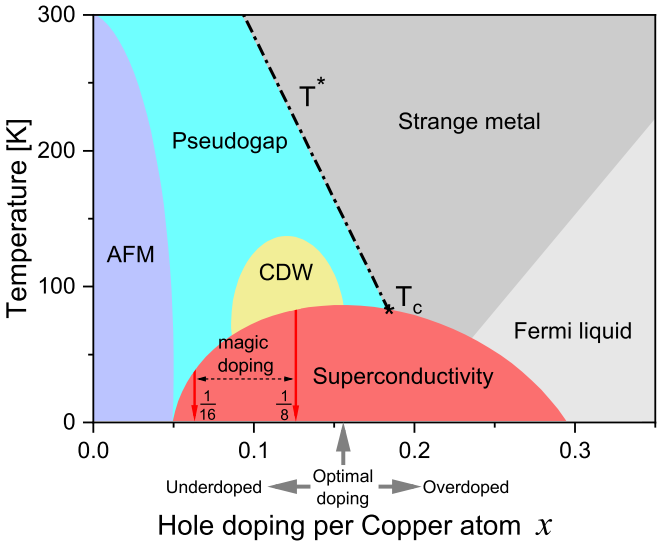

Figure 1: A illustration of hole doped cuprates phase diagram

Question One: With over 32 different classes and thousands of superconductors discovered [27], it is possible for almost all materials, including some insulators, to exhibit superconductivity under the right conditions, like an appropriate temperature and external pressure. In light of this, is it still reasonable to categorize superconducting materials into conventional and unconventional and to assume, subjectively, that they have distinct superconducting origins?

Question Two: The two vital experimental phenomena observed in all superconducting materials are zero resistance in an electric field [1] and the Meissner effect in a magnetic field

[28]. These experimental facts suggest that all superconductors, whether conventional or unconventional, must share the exact underlying mechanism of superconductivity. Moreover, opposite electric charges attracting each other is a universal law of nature, so isn't electromagnetic attraction the strongest and most suitable "glue" for pairings? Thus, the problem of superconductivity can be stated as a dynamic problem: how does the external electromagnetic field interact with the charge carriers inside the superconductor to induce the superconducting phase transition?

Question Three: Viewed through the Landau-Ginzburg phase transition theory [29], the order parameter characterizing the superconducting phase transition undergoes symmetry breaking. Therefore, it is clear that the transition is not spontaneous but instead is driven by an external field, resulting in a transition from high symmetry in the absence of an external field to a lower symmetry in its presence. The critical question when studying the mechanism of superconductivity is which electromagnetic variable qualifies as the order parameter in Landau-Ginzburg's theory.

Question Four: High-temperature superconductivity in copper-oxides is thought to originate from an antiferromagnetic parent Mott insulator, with electron localization spanning the entire range and a long-range order [30, 31]. On the one hand, strong magnetic excitations are generally believed to play a vital role in the superconducting mechanism [32–34]. On the other hand, the origin and nature of the magnetism underlying this phenomenon remain a mystery. To ultimately solve the high-temperature superconductivity mechanism, we must first successfully explain the reason for magnetism at the microscopic level. Therefore, a pivotal step toward explaining superconductivity is unraveling the nature of magnetism and elucidating the antiferromagnetic order within a localized electronic framework.

Question Five: It is widely acknowledged that existing superconducting theories and models are built on a dynamic view, where the movement of electrons drives current, supercurrent, and magnetic field phenomena. However, how can negatively charged electrons in a dense positive ion superconductor move freely without colliding? This decades-old unresolved issue leads us to propose that the picture of electron motion is at the root of the problem. To circumvent these difficulties, we suggest studying superconductivity using a static picture where all valence electrons are localized, which begs the question: is that even possible? We contend that the answer is yes, and it hinges on Maxwell's displacement current [35] and Dirac's magnetic monopole hypothesis [36]. Since the relationship between current and magnetic fields is mutual, these two theories are interchangeable - two different paths that lead to the same destination. Their common theoretical framework is static and does not depend on the motion of electrons to generate current or magnetic fields. Our primary task is to demonstrate that the two magnetic poles correspond precisely to electron and proton.

This paper presents a unified theory of superconductivity in real space, proposing an electron-proton electromagnetic interaction pairing mechanism that combines insights from the Mott insulator, Maxwell displacement current, and Dirac magnetic monopole theory. The theory elucidates the intrinsic relationships among superconductivity, magnetism, order parameters, and symmetry breaking without any extra glue. According to our proposal, the origin of natural magnetic phenomena can be traced back to the simplest possible electron-proton pair - a quantized vector capacitor - rather than the commonly assumed idea of electron motion. Furthermore, these electron-proton (ion) pairs can self-assemble into antiferromagnetic Mott insulators through direct electromagnetic interaction that results from attraction between oppositely charged particles. We demonstrate that the proton-electron electric dipole vector is precisely the order parameter for the Ginzburg-Landau theory of superconducting phase transition. The new mechanism can qualitatively and self-consistently explain many crucial superconducting phenomena, such as the Meissner effect [28, 37], London penetration depth [38], magic doping [39–41], vortex lattice [42–47], and vortex dynamics [48–54]. Additionally, our hypothesis perfectly encompasses the symmetry of Maxwell's equations [35], reveals the physical nature of electron spin [55], and offers insight into Dirac's magnetic monopoles [36].

II. ARE FREE ELECTRONS FREE?

In 1900, Drude proposed a theory to explain the transport properties of electrons in metals [56, 57]. Sommerfeld later refined the theory in 1927 by incorporating quantum mechanisms [58]. Despite the mathematical differences, the fundamental physical concepts have remained mostly unchanged. As depicted in Figure 2, these theories rely on the simplified model of a lattice of positive immobile ions (protons, for convenience) and valence electrons that are free to move. As illustrated in Figure 2, electrons (represented as the i-th electron in the figure) will continuously collide with ions and other electrons in random thermal movement inside the metal without an external electric field. However, under an applied electric field $\mathbf{E}$ along the $-x$ direction, as shown in Figure 2(b), the free electrons will exhibit a random directional motion, resulting in a drift velocity v_d in the opposite direction to conduct an electric current $\mathbf{I}$. The collisions between electrons and the lattice or other electrons induce resistance, thereby limiting the flow of electrons.

Intuitively, Drude's theoretical model contains several contradictions. First, the idea of electrons having a "tortoise-like" speed contrasts with the notion of current traveling at the speed of light, creating an inherent inconsistency. More fundamentally, the Drude model faces a serious challenge: how can positively charged ions that repel each other form a stable and symmetrical crystal structure in the presence of entirely disordered electrons? We will scrutinize the Drude model's rationality and reliability with current and energy as we delve further. As illustrated in Figure 2(b), the current flowing through a conductor follows the equation:

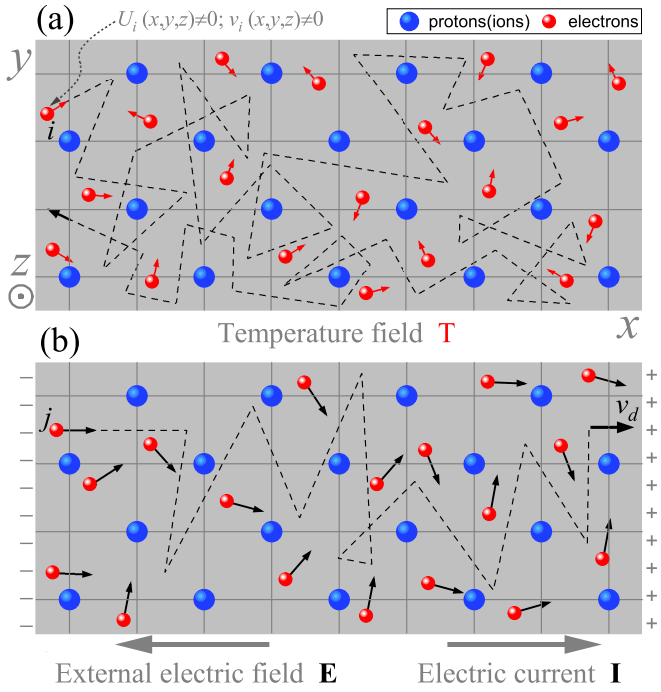

Figure 2: Drude free electron model and conductivity. (a) In the case of temperature $T > 0$ and no external electric field, the kinetic energy and potential energy of any valence electron in the conductor are not zero; (b) when applied an external electric field **E** on the metal, all electrons move directionally with a drift velocity v_d to generate an electric current **I**.

$$I = neS\bar{v}_d, \tag{1}$$

where n is the charge carrier (electrons) density, e is the electronic charge, S is the cross-sectional area of the conductor, and $\bar{v}_d$ is the average drift velocity.

In the case of direct current (DC), as shown in Eq. (1) and Fig. 3(a), the magnitude of the current **I** and the average drift velocity $\bar{v}_d$ of electrons remain constant in a uniform wire. This means the conductor has a continuous charge flow from one point to another and any given electron repeats the circuit cycle.

Regarding the alternating current illustrated in Figure 3(b), the current **I** oscillates periodically, and thus, so does the direction of the electron flow. This periodic inversion is physically impossible under Drude's free electron model. For instance, a 100 kHz AC current would necessitate that all the electrons inside the wire stop moving ($v_d = 0$) and reverse direction simultaneously every $0.01ms$. However, electrons possess inertia, and their velocities are diverse in magnitude and direction, as Drude suggested. Consequently, Drude's free electrons cannot immediately react to changes in the external electric field. High-frequency AC thus implies that electrons in an AC circuit do not move along with the current flow. As shown in Fig. 3(b), each electron acts like a harmonic oscillator, moving back and forth around its respective equilibrium position "0" with amplitude δ. This raises two critical

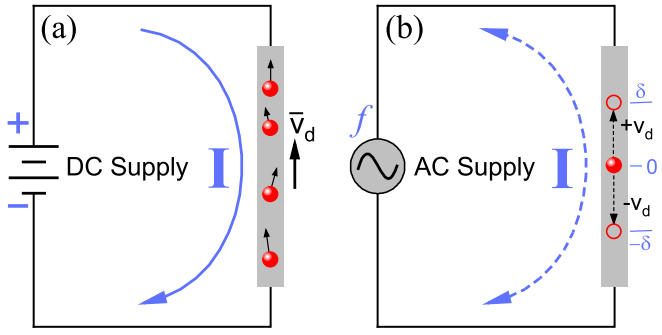

Figure 3: Drude's free electrons are not free. (a) In the case of DC, all Drude's electrons flow along the circuit, where electrons are in an extended state. (b) In the case of AC, electrons are confined to vibrate back and forth in a small space on the order of angstroms, where the electrons are in a bound state.

questions: (1) What is the order of magnitude of the amplitude δ? (2) Where are the equilibrium positions of the free electrons in the wire?

For the first question, we know that for copper $n = 8.5 \times 10^{28}/m^3$, let us assume a current of $3A$ that is flowing in a copper conductor with the wire diameter is 5 mm, by equation (1) we obtain $\bar{v}_d \sim 10^{-5} m/s$. When $f = 100$ kHz, the amplitude can be estimated as $\delta < \bar{v}_d/(2\sqrt{2}f) \sim 1\mathring{A}$. This result indicates that the alternating current electrons must be localized within a lattice constant. This result is very important since the transmission of alternating current can be realized only by micro displacement of electrons, so should direct current. Then the task is to find the respective equilibrium position for each electron in the metal.

The position of equilibrium is typically determined by minimizing the potential energy. In the case of Drude's free electron model, this potential energy is largely ignored due to the model's reliance on mean-field approximation and the removal of dominant electron-lattice interactions. To answer the second question, we need to consider the minimum free energy principle. As illustrated in Fig. 2(a), the energy of a free electron in a metal can be broken down into two components: kinetic energy resulting from free motion $v_i(x,y,z)$ and potential energy derived from the positive ion lattice $U_i(x,y,z)$. Therefore, we can define the overall free energy of electrons as:

$$E_{free} = \sum_i \left[\frac{m_e v_i^2(x,y,z)}{2} + |U_i(x,y,z)| \right], \tag{2}$$

where m_e is the mass of the electron.

It is not hard to see from Eq. (2) that when $v_i(x,y,z) = 0$, and $U_i(x,y,z) = 0$, we immediately have the minimum total free energy $E_{free} = 0$. Fig. 4 shows the candidate zero potential energy structure, known as Mott insulators. The yellow electron-proton (ion) electric dipole constitutes the most crucial repeating unit in the Mott-insulator-based electron-crystal model, containing hidden mysteries of nature. In Mott's

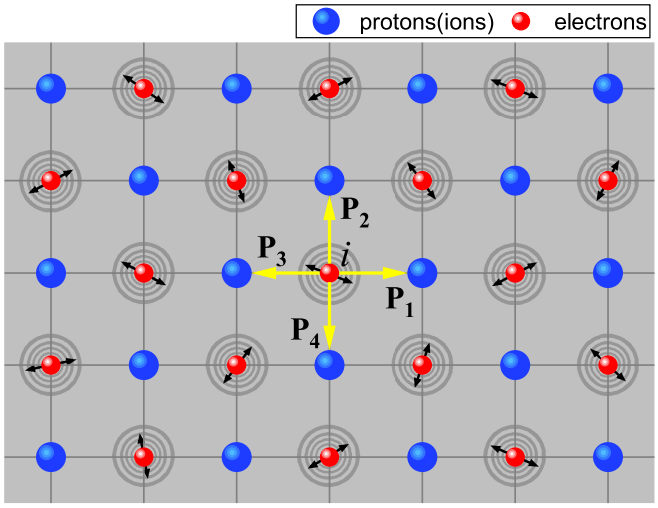

Figure 4: A Mott-insulator-based new electron-crystal model. There are no free electrons inside the material, and the electrons are trapped by the electric field of the surrounding ions (protons) and do thermal vibration in the equilibrium position. When $T = 0$, the crystal can be simplified to a symmetric proton-electron pair lattice, exactly the Mott insulator.

model, positively charged ions and negatively charged electrons form the same sublattice, representing a perfect unity of China's ancient philosophy of complementary "yin and yang" and modern Western science's minimum energy principle. The basis of "yin and yang" complementarity lies in equal rights, necessitating the formation of stable crystals comprising positive and negative charges that maintain mutual equality. The Drude model, by contrast, violates this principle by featuring unequal positive and negative charges, ultimately violating the minimum energy principle.

Although the Drude model of free electrons is widely used in condensed matter physics teaching and research, it presents significant challenges when extended to describe superconductivity. In the BCS framework, electrons in superconductors are assumed to flow without resistance at low temperatures, paired with opposite spins and momentum. However, this explanation raises concerns as it implies that these paired electrons, despite their random motions, can avoid electron-lattice and electron-electron collisions - a notion that seems unscientific. While some may ignore the physical mechanisms that guarantee the Cooper pairs maintain their spin and momentum opposites, it is impossible to overlook the continued existence of electron-ion attractive and electron-electron repulsive interactions. In particular, the coherence radius of Cooper pairs is much larger than that of a single electron, significantly increasing the collision probability between pair-pair and pair-lattice. Thus, BCS electron-pairing based on Drude's free electron postulates fails to eliminate the resistance of superconductors, in stark contrast, it dramatically increases resistance.

Figure 2(a) indicates that the Drude model suggests that the more impurities present in a conductor, the greater its resistance value. Consequently, impurities and defects do not decrease resistance or promote superconductivity, a notion that sharply contrasts with the phase diagram outlined in Fig. 1. Rather than increasing resistance, doping somehow causes the resistance to mysteriously vanish, particularly in the underdoped region, where increased impurities raise the superconducting transition temperature. Thus, a single, reasonable interpretation can account for this abnormal behavior: the current in metal wires and the supercurrents in superconductors do not rely on the directional motion of electrons. This conclusion is highly consistent with the previous discussion.

Free electrons are not free, and this is undoubtedly a revolutionary idea that will change many essential concepts in physics. It may seem common sense that electricity (or electric current) is an electromagnetic wave that travels at the speed of light and has almost nothing to do with the movement of electrons. Contrary to the description in the Drude model, the electrons in a wire do not have to travel long distances to carry electrical energy from one point to another. They only need to make a minor directed displacement from their initial equilibrium position to propagate an electric or supercurrent effectively. In the following sections, we will show in detail how our immobile-electric-charges hypothesis self-consistently explains the phase transition behavior between insulators, metals, semiconductors, superconductors, and magnets.

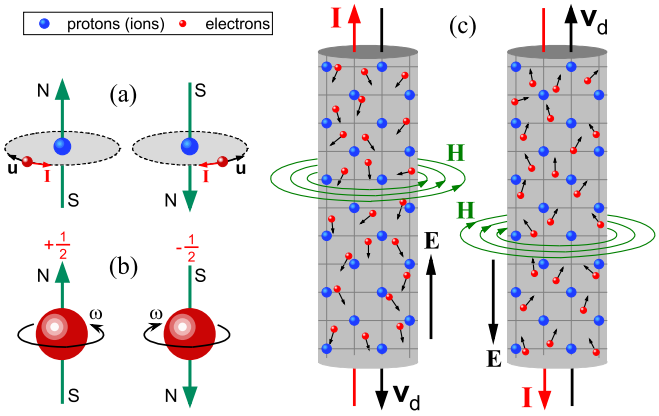

Figure 5: The traditional picture of magnetic fields induced by electron movement. (a) The orbital motion of electrons creates magnetic moments, (b) the electron spin hypothesis, (c) the electrons' upward and downward directed motion produces counterclockwise and clockwise magnetic fields, respectively.

III. THE MICROSCOPIC ORIGIN OF MAGNETISM

The history of magnetism dates back over 2,000 years to the Chinese invention of the compass. Today, modern physics posits that the essence of magnetism is rooted in the movement of electrons. As illustrated in Fig. 5, theoretical physicists suggest that electrons generate magnetic fields through

three distinct types of motion: (a) orbital circulation, (b) rotation, and (c) directional drift. Over time, numerous hypotheses and concepts have arisen to explain how electron motion generates magnetism, including the orbital magnetic moment, molecular current, spin, and current element.

Basic principles of electrodynamics suggest that electromagnetic wave emissions and energy loss typically accompany the movement of electrons. Therefore, sustaining the magnetic field depicted in Fig. 5 necessitates a constant influx of external energy to maintain electron motion. However, the existence of permanent magnetic materials in the universe contradicts this theoretical hypothesis, as their magnetic field intensity does not significantly decay over time. This objective fact refutes the notion of electron motion-induced magnetic fields, as depicted in Fig. 5. In addition, the duality between electric and magnetic fields implies that generating a magnetic field requires static magnetic charges, as Dirac recognized when he proposed the theory of magnetic monopoles [36].

A. What are magnetic monopoles?

Is there a presence of static magnetic monopoles in nature? This question not only concerns the symmetry of Maxwell's equations but also has the potential to significantly disrupt the foundational principles of physics that are built on magnetic fields created by moving charges. If magnetic monopoles were to exist, it could indicate that our understanding of magnetism, which has been developed over millennia - including Figure 5 - is fundamentally flawed. Moreover, it would require the revision of scientific theories and theoretical explanations of superconductivity, such as the BCS theory that scientists have developed over the past century.

Since Dirac formulated his theory, many attempts have been made to discover the mysterious new particles he predicted - magnetic monopoles. However, researchers have yet to find conclusive evidence of their existence even after almost a century of searching. In ancient Chinese poetry, a verse roughly translates to "In a crowd, I search for her in vain, but when I turn my head, I find her where the lantern light is dimly shed." This begs the question: Could it be possible that the magnetic monopoles we are trying to find are simply another manifestation of the well-known elementary particles? In the following discussion, we will put forth a possible answer to this question. Dirac proposed that electric and magnetic charges could coexist and satisfy the following quantization condition:

$$eg = \frac{hc}{4\pi}n = \frac{\hbar c}{2}n, \tag{3}$$

where e and g are the electric and magnetic charges, respectively, h is the Plank's constant [59], and n being the integers.

What is incredible is that the seemingly simple formula (3) hides the secret of the origin of the magnetism of materials. Using the fine structure constant $\alpha = e^2/4\pi\varepsilon_0\hbar c$, the Dirac's formula of Eq. (3) can be re-expressed as:

$$g = (\frac{n}{8\pi\varepsilon_0\alpha})e = \Pi_n e, \tag{4}$$

where Π_n is an adjustable constant.

The relation presented in Eq. (4) above provides us with a clear understanding that the supposed magnetic monopoles are, in fact, just dressed electrons or protons. This implies that the superimposed electric field created by the electron-proton pair is, in reality, the magnetic field. It is intriguing to note that electrons and protons can simultaneously serve as electric and magnetic charges. In the following sections, we shall employ Maxwell's theory to verify that the positive and negative magnetic poles correspond to protons and electrons.

B. Vector capacitor, displacement current and magnetic field

As shown in Figs. 6(a) and (b), for an isolated electron or proton, they will generate electric fields $\mathbf{E}_-$ and $\mathbf{E}_+$ respectively. Assuming that the electron and proton coincide with each other with the spacing $r = 0$, as illustrated in Fig. 6(c), due to their perfect symmetry, there is no electromagnetic field in the space around them. When $r \neq 0$, the electron and proton will form an electric dipole through symmetry breaking. It is well known that a proton-electron pair is not just an electric dipole, it can also be a hydrogen atom or a neutron. Moreover, as shown in Fig. 6(d), in metal wires, proton-electron pairs are the smallest capacitance in nature, they are quantized vector capacitors with directional characteristics, and their capacitance can be determined by $C_r = 2\pi\varepsilon_0 r$ (where r the

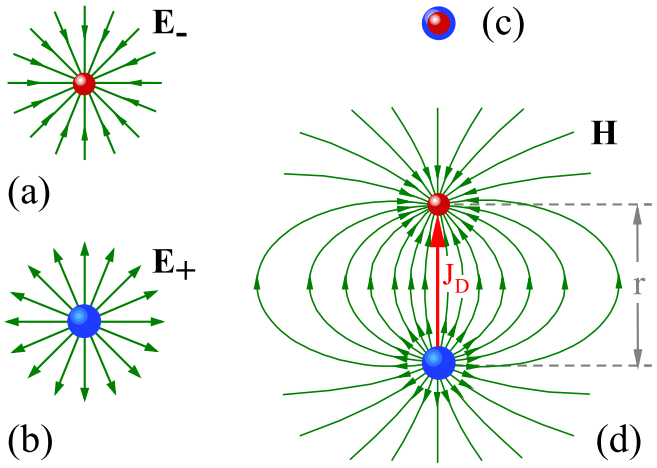

Figure 6: A new magnetic mechanism based on Dirac's theory of magnetic monopoles. (a) and (b) The electric field of an isolated electron and proton, respectively, (c) when the coordinates of the electron and proton coincide, their associated electric fields (or magnetic field) are hidden, (d) an electron-proton pair (a quantized vector capacitance) creates a displacement current density and an associated magnetic field.

distance of the electric dipole). According to Maxwell's theory, a displacement current density $\mathbf{J}_D = \varepsilon_0 \partial \mathbf{E}/\partial t$ exists in the capacitor, which will create an associated magnetic field in the surrounding space. In other words, the electron-proton pair produces the excited magnetic field, and this conclusion is entirely consistent with Eq. (4). Then, the magnetic field strength $\mathbf{H}$ of the electron-proton pair can be defined and determined by Maxwell's statement: a changing electric field produces a magnetic field.

When the electric field $\mathbf{E}_+$ of a positive proton and the electric field $\mathbf{E}_-$ of a negative electron simultaneously appear in the surrounding space, since the two electric fields are of opposite signs, their superposition represents the changing electric field. Hence, according to Maxwell's hypothesis, the vector superposition of electric fields $\mathbf{E}_+$ and $\mathbf{E}_-$ is precisely the magnetic field $\mathbf{B}$, which is given by

$$\mathbf{B} = \mu_0 \mathbf{H} = \frac{\mathbf{E}_+ + \mathbf{E}_-}{c}, \tag{5}$$

where c is the speed of light and μ_0 is the vacuum permeability.

Based on the discussion presented above, it is apparent that in the previous framework depicted in Fig. 5(b), the electron spin was considered an intrinsic form of angular momentum [55], which was perceived to be a purely quantum mechanical concept. However, experimental evidence has yet to prove that free electrons have spin. This is highlighted by experiments such as the atomic fine spectral structure experiments [60] and the Stern-Gerlach silver atom beam experiment [61], which demonstrate the spin magnetic moments of atoms such as silver or hydrogen, rather than free electrons. In the new framework of symmetry breaking, it is intriguing to discover that the concept that free electrons possess no spin is hidden in Eq. (5). This formula suggests that an isolated electron can only create an electric field and that there is no inherent notion of a spin moment. Within atoms, electrons couple with protons to generate an electric dipole as depicted in Fig. 6(d), which possesses magnetic moment properties and is now envisioned as electron spin within modern physics. Spin can be visualized as a coat that surrounds electrons, with naked electrons lacking any spin properties. The phenomenal occurrence of charge-spin separation can be observed in some superconductors.

C. Magnetic field of electrified wire

Accordingly, the question that arises is how the new theory explains the magnetic field generated by the current-carrying wire in the surrounding space as shown in Fig. 5(c)? To see why, let us look at Fig. 7, a schematic representation of the generation of magnetic fields solely through the spatial symmetry breaking of electron-proton pairs. As shown in Fig. 7(a), in the absence of an external field, the positively charged

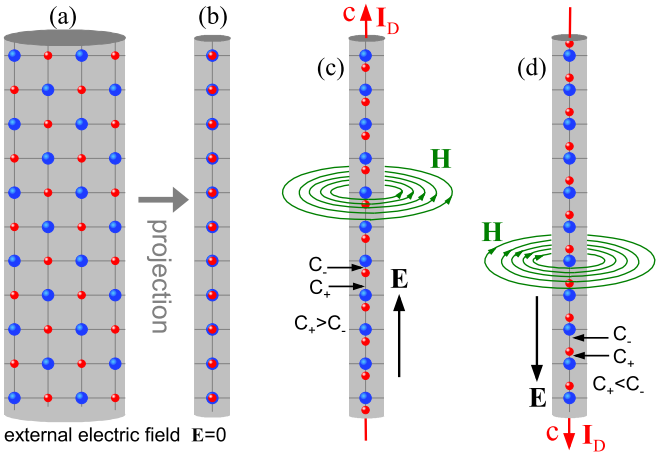

Figure 7: The illustration of how the wire's static electric dipoles generate the magnetic fields. (a) and (b) In the absence of an external electric field and regardless of the influence of temperature, the electromagnetic fields of positive and negative charges are hidden due to the symmetry of the internal structure, so there is no external electric field or magnetic field outside the conductor. (c) and (d) The applied electric field causes the electrons to deviate from the equilibrium position and the symmetry-breaking phase transition, and the upward and downward electric fields will induce counterclockwise and clockwise magnetic fields, respectively.

ions (protons) and electrons inside the wire form a Mott insulating lattice, which can be projected as a simple quasi-one-dimensional structure of Fig. 7(b), and there is no magnetic field around the wire due to the high symmetry of the electron-proton pairs. As shown in Figs. 7(c) and (d), when an external electric field is applied upwards or downwards along the wire, the electrons in the wire will deviate from the equilibrium position downwards or upwards, respectively, under the action of the electric field. Such Peierls-like symmetry-breaking transition results in a net capacitance $C_{net} = C_+ - C_-$. When the electric field is upward, then $C_{net} > 0$, while the electric field is downward, then $C_{net} < 0$. As illustrated in the figure, this transition leads to the induction of magnetic fields $\mathbf{H}$ in counterclockwise and clockwise directions around the conductor and displacement current $\mathbf{I}_\mathrm{D}$ up and down along the conductor.

In light of the preceding discussions, we can recognize two distinct sources of magnetism, with the old explanation entirely dependent on time-dependent continuous electron movement, while the new explanation relies upon the time-independent electric dipole or capacitor formed from electron-proton pairs. Based on the principle of minimum energy and the earlier analysis, the concept of perpetual electron movement generating a magnetic field lacks scientific foundations. It follows that the proton-electron pair magnetism proposed in this paper, which originates from Dirac's magnetic monopole and Maxwell's displacement current hypotheses, is much more reasonable and plausible as a natural choice.

IV. SYMMETRY OF MAXWELL'S EQUATIONS

The differential form of the Maxwell's equations can be written as:

$$\begin{aligned} \nabla \cdot \mathbf{E} &= \frac{\rho_e}{\varepsilon_0}, \\ \nabla \cdot \mathbf{B} &= 0, \\ \nabla \times \mathbf{E} &= -\frac{\partial \mathbf{B}}{\partial t}, \\ \nabla \times \mathbf{B} &= \mu_0(\mathbf{J}_D + \mathbf{J}_e), \end{aligned} \tag{6}$$

where $\mathbf{E}$ is the electric field, $\mathbf{B}$ is the magnetic field, ρ_e is the electric charge density, $\mathbf{J}_e$ is the electric current density, and $\mathbf{J}_D = \varepsilon_0 \partial \mathbf{E}/\partial t$ is the displacement current.

Maxwell's equations of Eq. (6) is considered the most beautiful and elegant formula in physics. Because it is not mathematically perfect symmetry, significant efforts have still been made to achieve the exact symmetry of the equations, including Dirac's magnetic monopole hypothesis [36]. It should be pointed out that it is not the right way to realize the symmetry of the equation through mathematical skills or artificial hypotheses of new particles. In the previous section, we have obtained three significant findings: (I) the conduction current that relies on the movement of electrons does not exist, (II) the magnetic field is produced by the proton-electron electric dipole of Eq. (5), (III) the magnetic monopoles of Eq. (4) are the isolated electrons and protons.

With the above new findings, we can now reconsider the symmetry of Maxwell's Equations. Maxwell's first equation of Eq. (6) is based on Gauss' law, which describes the electrostatic field. The second equation of Eq. (6) is based on Gauss's law on magnetostatics. Here, we will show that these two equations are intrinsically related, and the second equation can be derived from the first equation. For a proton-electron pair with the electric dipole vector $\mathbf{P}$, according to the first equation of Eq. (6), the electric field generated by the pair satisfies:

$$\nabla \cdot (\mathbf{E}_+ + \mathbf{E}_-) = \frac{[\rho_e(\mathbf{r}_p) + \rho_{-e}(\mathbf{r}_p + \mathbf{P}/e)]}{\varepsilon_0}, \tag{7}$$

where e is the electron charge, $\mathbf{r}_p$ is the coordinate position of the proton, $(\mathbf{E}_+, \rho_e)$ and $(\mathbf{E}_-, \rho_{-e})$ are the electric fields and the electric charge densities of proton and electron, respectively.

Substituting Eq. (5) into Eq. (7) , we have

$$\nabla \cdot \mathbf{B} = \frac{[\rho_e(\mathbf{r}_p) + \rho_{-e}(\mathbf{r}_p + \mathbf{P}/e)]}{c\varepsilon_0}. \tag{8}$$

Usually, $\mathbf{P}/e$ is an infinitesimal length (far less than an Ångström), under a far-field approximation $\mathbf{r}_\mathrm{p} + \mathbf{P}/e \simeq \mathbf{r}_\mathrm{p}$, it is reasonable to assume that proton and electron nearby of each other, or $\rho_e(\mathbf{r}_p) + \rho_{-e}(\mathbf{r}_p + \mathbf{P}/e) \simeq 0$, then Eq. (8) will approximately become the second Maxwell's equation. This result means that Maxwell's second equation is not strictly true, or the right-hand side of the equation is not exactly zero. Furthermore, our conjecture has ruled out the existence of conduction currents, this means that $\mathbf{J}_e$ in the fourth Maxwell equation must be equal to zero. So far, we have developed all the tools necessary to rewrite the Maxwell equations. The new equations can be given immediately as:

$$\begin{aligned} \nabla \cdot \mathbf{E} &= \frac{\rho_e}{\varepsilon_0}, \\ \nabla \cdot \mathbf{B} &\simeq 0, \\ \nabla \times \mathbf{E} &= -\frac{\partial \mathbf{B}}{\partial t}, \\ \nabla \times \mathbf{B} &= \mu_0 \varepsilon_0 \frac{\partial \mathbf{E}}{\partial t}. \end{aligned} \tag{9}$$

Compared to Maxwell's equations in Eq. (6), the new equation in Eq. (9) has made two important breakthroughs. Firstly, it can be observed that the original first and second equations in Eq. (6) are entirely independent and uncoupled, which means that Maxwell's equations have not fully achieved the unification of electrical and magnetic phenomena. However, the new first and second equations in Eq. (9) are intrinsically interrelated; the first equation depicts the electric field generated by unpaired charges (protons or electrons), while the second equation describes the magnetic field generated by paired charges. Secondly, the presence of excess conduction current $\mathbf{J}_e$ renders the original third and fourth equations of Eq. (6) unsymmetrical. The absence of conduction current results in the natural realization of the symmetry of the new third and fourth equations.

V. ANTIFERROMAGNETISM, ORDER PARAMETERS AND MAGIC DOPING

The antiferromagnetic Mott insulator has garnered significant attention for its potential to unravel the mysteries of high-temperature superconductivity. However, the dominant theoretical explanation of high-temperature superconductivity in the past few decades utilized the Hubbard and extended Hubbard models [21, 22, 62]. We want to point out that these models were based on a misunderstanding of the nature of magnetism and antiferromagnetism. Therefore, why Mott insulators possess strong antiferromagnetic correlations still necessitates an explanation. In light of this, our paper proposes the proton-electron paired magnetic dipole hypothesis. Our hypothesis establishes a novel understanding of the phenomenon in question, and this question is no longer a mystery.

A. Excited state and magnetic moment of electrons

The electrons in a Mott insulator can be considered identical particles in the ground state. As shown in Fig. 8, we present a two-dimensional Mott insulator phase with square symmetry. In Fig. 8(a), we use four degenerate electric dipole

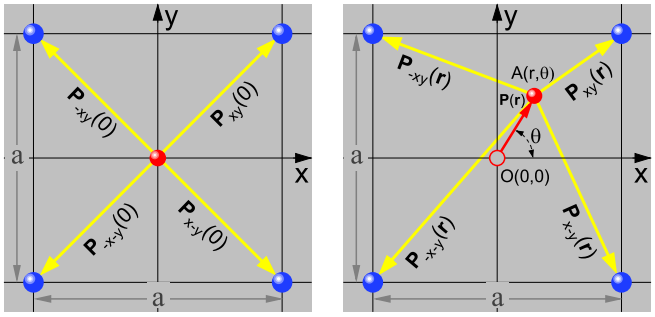

Figure 8: The electric dipole vector represents two electronic states in a two-dimensional square lattice. (a) Mott insulating ground state; (b) excited state.

vectors to describe it. These four electric dipoles can be integrated into a total vector as:

$$\begin{aligned}\mathbf{P}_G &= \mathbf{P}_{Mott} \\ &= \mathbf{P}_{xy}(0) + \mathbf{P}_{-xy}(0) + \mathbf{P}_{x-y}(0) + \mathbf{P}_{-x-y}(0) \\ &= 0.\end{aligned} \tag{10}$$

Under the influence of external factors such as temperature, pressure, and electromagnetic fields, the ground state electrons in Fig. 8(a) will deviate from the equilibrium position and enter the excited state. Correspondingly, the Mott-insulating state will transition into a metallic, magnetic or superconducting state according to external conditions. As shown in Fig. 8(b), when the electron occurs transition from ground state $O(0,0)$ to excited state $A(r,\theta)$ with a vector $\mathbf{P}(\mathbf{r}) = e\mathbf{r}$ marked by the red arrow, the corresponding electric dipole vector $\mathbf{P}_{\mathrm{E}}$ can be expressed as the superposition of four new electric dipole vectors . Using formula (10), we can get the following relationship:

$$\begin{aligned}\mathbf{P}_{\mathrm{E}} &= \mathbf{P}_{xy}(\mathbf{r}) + \mathbf{P}_{-xy}(\mathbf{r}) + \mathbf{P}_{-x-y}(\mathbf{r}) + \mathbf{P}_{x-y}(\mathbf{r}), \\ &= \mathbf{P}_{\mathrm{G}} - 4\mathbf{P}(\mathbf{r}), \\ &= -4\mathbf{P}(\mathbf{r}).\end{aligned} \tag{11}$$

Assuming that the positive ion lattice has not changed before and after the phase transition, the physical quantity $\mathbf{P}_{\mathrm{E}}$ of Eq. (11) is only related to the displacement vector $\mathbf{r}$ of the electron. In this case, the physical system of Fig. 9(a) can be simplified as Fig. 9(b), where the $\mathbf{P}_{\mathrm{E}}$ can be completely endow to the electrons with the intrinsic quantized magnetic vector:

$$\mathbf{P}_m = \Gamma(\mathrm{c,h})\mathbf{P}_{\mathrm{E}} = p_m(r)\exp(i\theta), \tag{12}$$

where Γ(c,h) is the proportional constant related to the speed of light c and Planck constant h.

The emergence of the magnetic vector $\mathbf{P}_m$ indicates the excitation of the hidden magnetic state of the superconducting parent, equivalent to inducing a magnetic moment in the opposite direction to $\mathbf{P}(\mathbf{r})$. This elementary excitation process leads to the destruction of the Mott long-range antiferromagnetic phase. The magnetic vector can function as the spin

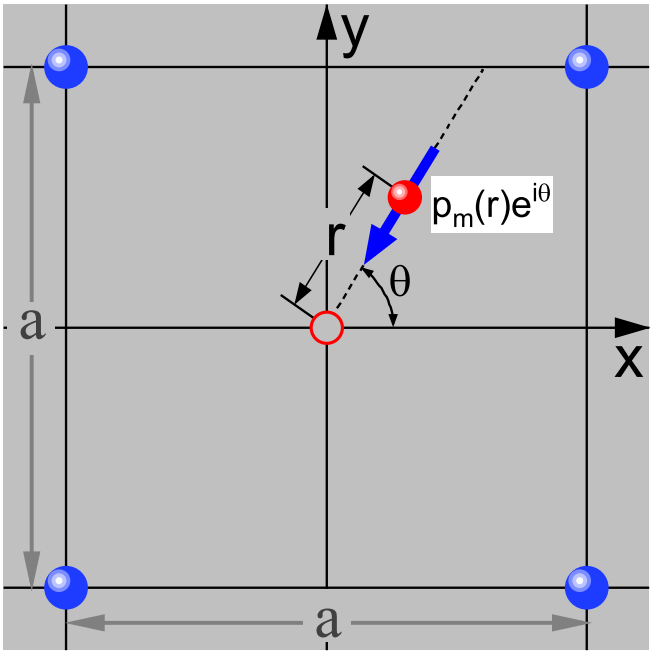

Figure 9: The excited electron state in Fig 8(b) can be simplified as a magnetic vector $p_m(r)e^{i\theta}$.

and magnetic moment of the excited electrons and serves as the order parameter of the Ginzburg-Landau phase transition theory. Notably, an electron's magnetic properties are not inherent but stem from the interaction with positively charged lattices. Once electrons depart from the material and become free, their magnetism, or spin, vanishes instantaneously. As such, it is now evident that electrons do not inherently possess the so-called intrinsic spin, which explains the phenomenon of charge-spin separation observed in experimentss [63].

B. Order parameters and symmetry breaking

Undoubtedly, the Ginzburg-Landau phase transition theory is currently the most successful theory of superconductivity [29]. As a phenomenological theory, it captures the two primary elements of superconducting phase transition: the order parameter and symmetry breaking. However, Landau's theory requires further development as it cannot address the fundamental question on the microscopic level: What constitutes the order parameter with electromagnetic properties? It is evident that the proton-electron electric dipole moment underpins the order parameter in Ginzburg-Landau's theory. Thus, our proposed theory specifies and completes Landau's theory by identifying the essential nature of the order parameter.

In condensed matter physics, phase transitions in materials are accountable for the modifications in their physical properties. The evolution of a symmetry-breaking order parameter delineates these transitions. As the proton-electron electric dipole can play an integral role in the order parameter, it is essential to provide a unified microscopic explanation of the

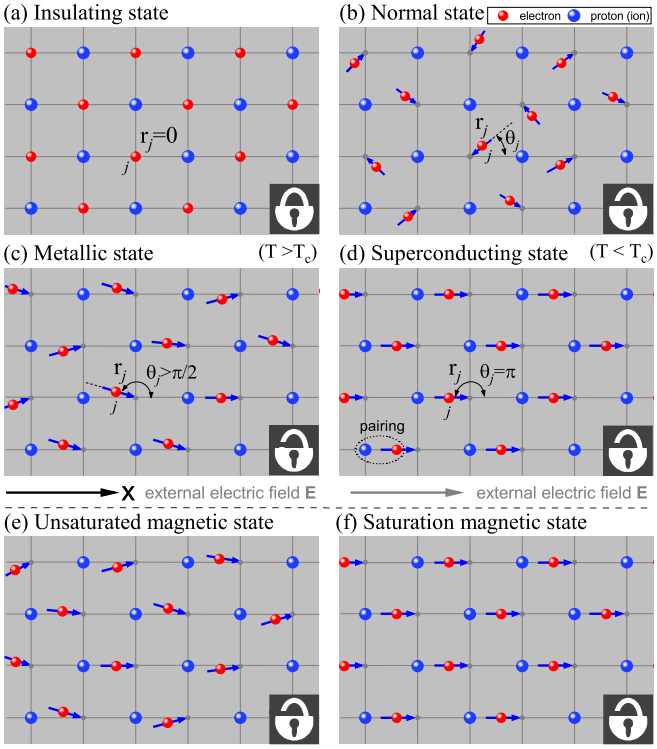

Figure 10: Five typical condensation states based on symmetry and symmetry-breaking. (a) The insulating state with the highest symmetry of perfect crystal; (b) the normal state with a complete disorder of magnetic vector orientation; (c) the external field-induced metallic state associated with quasi-parallel magnetic vectors at $T > T_c$; (d) the quantum superconducting state that occurs at $T < T_c$ when all magnetic vectors become coherent and align strictly along the direction of the electric field; (e) and (f) the unsaturated and saturated magnetic states, respectively, which may occur spontaneously or be induced by external magnetic fields. Note that in the insulating state (a), the electrical and magnetic properties of materials are locked (hidden) due to symmetry. When symmetry is broken, the electromagnetic properties become unlocked and excited.

phase transitions observed in various materials, such as superconductivity, insulators, magnetic and metallic materials. For a conductor containing N valence electrons, from Eq. (12), we can define the order parameter of the conductor as follow:

$$\mathbf{P}_{order} = \sum_{j=1}^{N} p_m(r_j) \exp(i\theta_j) \tag{13}$$

By using Eq. (13), it is possible to distinguish among five typical condensed states and display their essential differences at the microscopic scale. First, as shown in the Fig. 10(a), when $r_j = 0$, then $p_m(r_j) = 0$ and the order parameter $\mathbf{P}_{order} = 0$, this is the insulating state in which no symmetry breaking occurs, and the symmetry of the electrons exactly matches the symmetry of the lattice. In the second case of Fig. 10(b), r_j is a small random displacement of the j-th electron from its equilibrium as a result of random thermal fluctuations. Since the orientation order parameter θ_j is isotropic, from Eq. (13) we immediately have $\mathbf{P}_{order} = 0$. It must be pointed out that although the order parameter $\mathbf{P}_{order}$ in Figs. 10(a) and (b) are both equal to zero, their corresponding physical systems are entirely different, the former is an insulating state and the latter is a normal state (or disordered state).

Fig. 10(c) shows the third case of the metallic state. Suppose the external electric field is applied alone x axis, all electrons will collectively shift from around the equilibrium positions to the left. Due to the influence of random thermal motion, the system is non-completely broken symmetry. In this case, the dominated component of the order parameter appears in the x-direction of the electric field. As a result, in addition to the main electromagnetic energy flow in the x-direction characterized by an electric current. There is energy loss in the direction perpendicular to the electric field, which contributes to the resistance.

Figure 10(d) depicts the fourth case of the superconducting state when $T < T_c$, the thermal disturbance is almost completely suppressed, and the order parameter is strictly along the direction of the electric field. In this case, the orientation angle in Eq. (13) is the same as $\theta_j = \pi$, the system has perfect symmetry breaking, and all electrons condense coherently into a single quantum state with a zero resistance. It should be noted that there is no distinction between conventional and unconventional superconductors under our theoretical framework. The stability of the order parameter $\mathbf{P}_{order}$ mainly determines the superconducting transition temperature. Because the lattice constant of elementary superconductors is relatively small, the strong repulsive interaction between electrons leads to the instability of the order parameter $\mathbf{P}_{order}$, which in turn makes T_c lower. In contrast, the lattice constant of high-temperature superconducting materials is generally large and $\mathbf{P}_{order}$ is much more stable than that of low-temperature superconductors. Furthermore, high pressure can influence the superconducting transition temperature, and the pressure effect on the T_c can be positive or negative. These experimental results can also be qualitatively explained in Fig. 10(d). On the one hand, pressing reduces the lattice constant, which leads to a decrease in T_c, on the other hand, it increases the stability of the whole lattice and improves T_c. Hence, the pressure effect on superconducting properties involves the competition of two distinct structural phase transitions.

Apart from the four states mentioned above, the magnetic state is another essential natural phenomenon closely related to the metallic and superconducting states. Figures 10(e) and (f) display unsaturated and saturated magnetic states, respectively. Their microstructures are entirely consistent with those of metallic and superconducting states displayed in Figs. 10(c) and (d), correspondingly. Their differences stem from external factors such as temperature, electric, and magnetic fields that induce the phenomenon. Our theory suggests that three primary types of related complete symmetry-breaking phenomena of electronic states in nature exist. The first type is the superconducting state of Fig. 10(d) induced by the electric field and temperature combination. The second type is the magnetic state of Fig. 10(f) induced only needs to be low-

ered to a proper temperature (the Curie temperature), and the third type is the superconducting Meissner effect induced by the combination of magnetic field and temperature. It must be emphasized that the micro-physical mechanisms of these three seemingly completely different phenomena are precisely the same, all due to the symmetry breaking of electronic structure related to Peierls phase transition. Permanent magnet materials are spontaneous symmetry-breaking phase transitions, while superconductivity is a symmetry-breaking phase transition driven by an external field.

It is worth noting that our theory is also based on pairing, as shown in Figure 10(d). However, it significantly differs from the phonon-mediated pairing process of identical nonlocal charges (i.e., electrons and electrons) described in the BCS theory. Instead, our theory relies on the electromagnetic interaction between two different localized charges (i.e., electrons and protons) in real space, leading to a non-quasiparticle attractive pairing mechanism.

Referring to Fig. 1, the typical phase diagram of copper oxide high-temperature superconductor is complex, encompassing most of the primary phenomena investigated in solid-state physics. Based on our discussion in this section, a significant conclusion can be drawn: the Mott insulator forms the basis of superconductors, metals, magnets, and semiconductors. From a microscopic perspective, the primary disparity among different physical phases portrayed in Fig. 1 lies in the distinct orientation order of the electric dipole composed of electrons and protons (ions).

C. Magic doping and chessboard structure

Most known cuprate superconductors are composed of three stable phases: the insulating antiferromagnetic phase, the superconducting phase, and the metallic phase, depending on the concentration of doped carriers. In certain cuprate compounds, such as $La_{2-x}Sr_xCuO_4$ (LSCO), $Ca_{2-x}Na_xCuO_2Cl_2$ (NCCOC), and $Bi_2Sr_2CaCu_2O_{8+\delta}$ (BSCCO), there exist some charge-ordered states that have been observed to compete with superconductivity. Theoretical studies predict that 2D chessboard charge ordering patterns can be observed at the magic doping fraction $x = x(m, n) = (2m + 1)/2^n$, where m and n are integers [41].

The existence of localized electron competition phases below the superconducting transition temperature is an experimental fact sufficient to challenge traditional superconducting theories' fundamentals. In the following section, we will use the magical doping results directly to scrutinize the rationality of electron Cooper pairing and resistive superconducting current, as recognized by superconducting scholars. To achieve this, we can acquire three LSCO superconducting samples with doping concentrations of $x = 0.124$, 0.125, and 0.126, respectively. All three samples are placed under cooling to T_c, and the results show that the first and third samples exhibit superconductivity while the second sample does not. This prompts us to question why superconductivity is

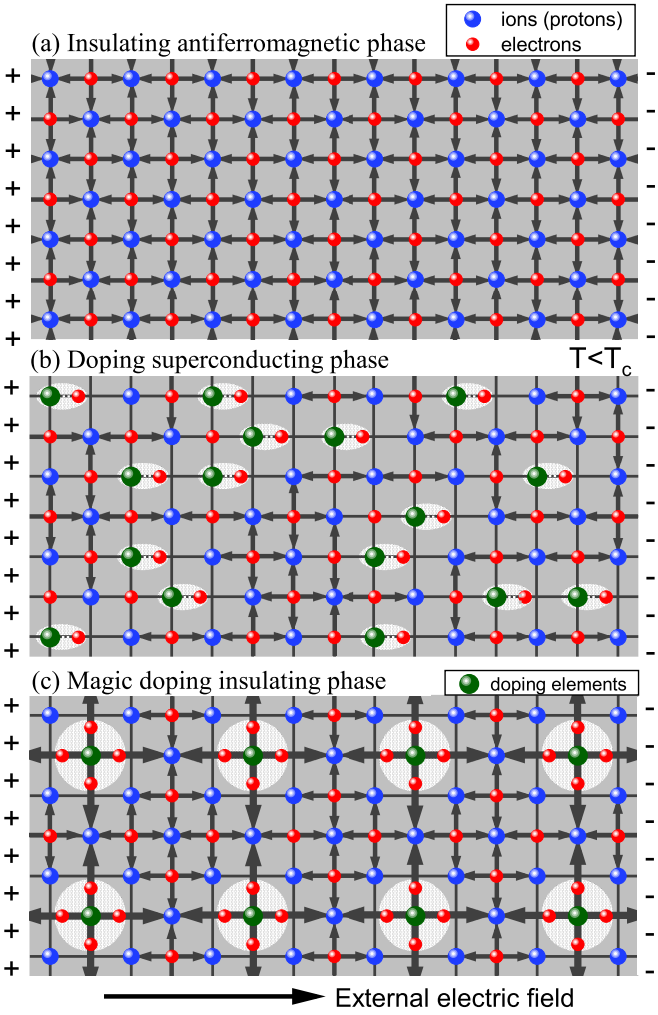

Figure 11: Comparison between cuprate high-temperature superconducting state and magic doping insulating state. (a) Shows the parent Mott insulator with antiferromagnetic order; (b) depicts the doped superconducting state, where the long-range antiferromagnetic order is destroyed.; (c) illustrates the insulating chessboard structure at the magic doping level, where the antiferromagnetic order remains after renormalization.

so profoundly affected by alterations in doping concentration. Clearly, the old superconducting pairing mechanism is unable to offer any explanation for this phenomenon. As a newly established superconducting theory presented in this paper, it is imperative first to explain these unique cases of magical doping occurrence.

Both the antiferromagnetic Mott insulating phase and the magic doping insulating phase suggest that the superconducting mechanism must be established on a localized electronic picture, as discussed in the previous sections. As illustrated in Figure 11, our theory presents the microscopic electronic states evolution process of cuprate superconductors, from the parent insulating state to the doped superconducting state and then to the magic doping insulating state. In the undoped Mott parent compound in Fig. 11, strong electron-ion coupling

prevents the displacement of electrons by an external electric field, and the symmetry breaking of the order parameters results in a long-range antiferromagnetic insulating state. When ions are partially replaced and carriers are randomly doped in Fig. 11, the pairing of some local electrons and ions becomes significantly weakened. Consequently, these electrons can be displaced under an external field, resulting in symmetry breaking and the emergence of superconductivity. In the case of magic doping in Fig. 11, some ions are regularly replaced with a chessboard structure, forming locally symmetric electronic states around the ions. After renormalization, the system retains long-range antiferromagnetic order. Therefore, the external electric field cannot realize superconducting phase transition by destroying the symmetry of electronic states.

It is crucial to note that the diagrams displayed in Figs.11 depict a simplified two-dimensional model. In reality, for three-dimensional copper-based high-temperature superconductors, the changes in electron states observed in the copper-oxygen layers can be attributed to doping ions originating from adjacent layers.

D. One-dimensional superconductivity

Many superconductors possess quasi-two-dimensional crystal structures but exhibit one-dimensional characteristics, such as spin-charge separation [63], stripe phases [64, 65], and spin and charge fluctuations [66]. Because of the simplicity of one-dimensional systems, investigating the superconducting properties of quasi-one-dimensional electron correlation systems is expected to aid in uncovering the mechanism of high-temperature superconductivity. The most significant aspect of discovering one-dimensional superconductivity is its complete rejection of the hypothesis of free electrons as a bedrock of traditional superconductivity theories. Inversely charged electrons cannot move (or hop) within a positive charge chain without loss. The most probable outcome is that they are confined within potential energy traps and become localized electrons. Therefore, two meaningful questions arise: (1) do quasi-one-dimensional superconductors exist? (2) How is superconductivity achieved in them?

We can answer these two questions through Figure 11(b). It can be seen from the figure that after the Mott insulator is doped in disorder, those electrons affected by doping will transition from the ground state to the excited state under the action of an external field and cause local and global symmetry breaking. The excited electrons in the figure can be re-represented by capacitance as the parallel quasi-one-dimensional vector capacitance array in Fig. 12. The superconducting displacement current $\mathbf{I}_D$ propagating at the speed of light can propagate lossless in a quasi-one-dimensional capacitor chain. Because an electron's position (that is, the charge) moves at a much slower speed than the change speed of the magnetic moment (or spin) it excites, there will be an observed phenomenon of charge-spin separation.

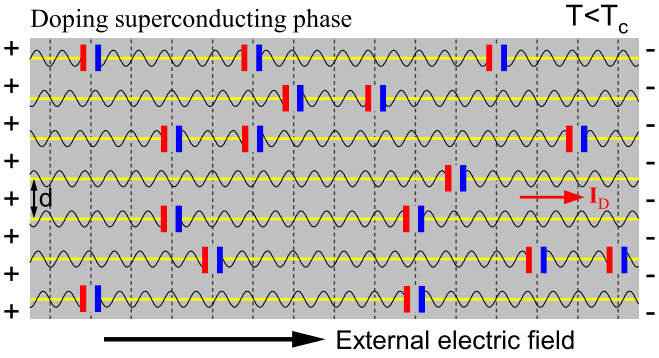

Figure 12: Figure 11(b) is re-represented using vector capacitance, and the quasi-one-dimensional vector capacitor chains supports the existence of one-dimensional superconductivity [67].

The Fig. 12 clearly shows that the stability of the orientation of the quasi-one-dimensional vector capacitor chain directly impacts the superconducting transition temperature. A larger chain spacing (d) leads to a more stable capacitor chain, producing a higher superconducting transition temperature. It is important to note that even traditional elemental superconductors also rely on the displacement current of vector capacitors for electricity conduction. However, their relatively small chain spacing generally results in a lower superconducting transition temperature.

VI. MEISSNER EFFECT PUZZLE

Besides exhibiting zero resistivity, superconductors are also characterized by impeccable diamagnetism, referred to as the

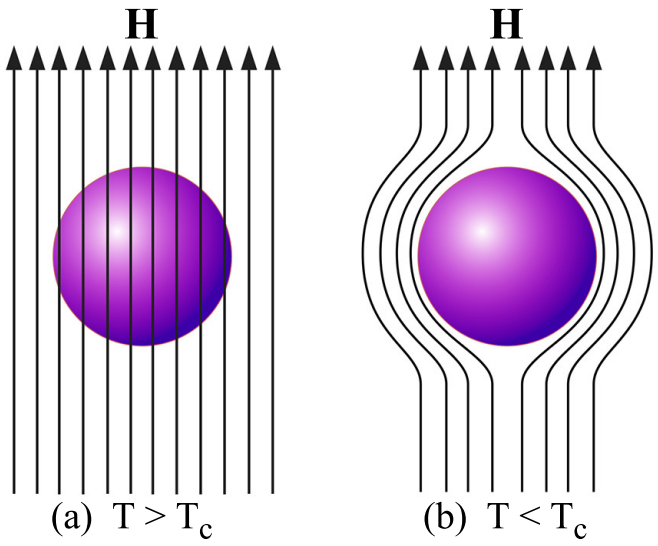

Figure 13: The mainstream explanation of the Meissner effect: (a) above the critical temperature, the magnetic field is able to penetrate the superconductor, (b) below the critical temperature, the magnetic field is excluded from the interior of the superconductor.

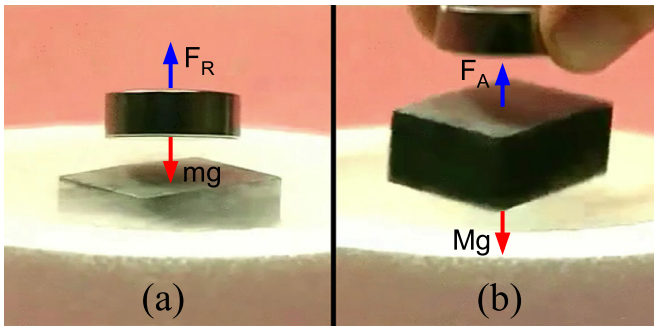

Figure 14: The Messner effect experiment video of Ref. [37] includes two screenshots: (a) depicting a strong repulsion between the superconductor and magnet, causing the magnet to levitate, and (b) depicting a strong attraction between the superconductor and magnet, resulting in the levitation of the superconductor.

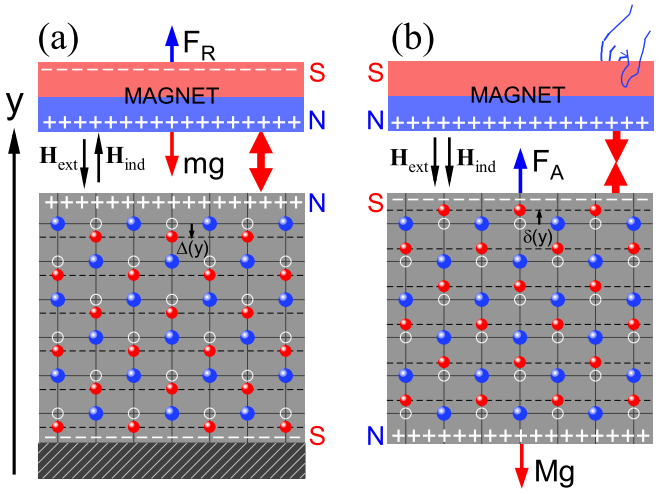

Figure 15: Schematic explanation of Meissner effect experiment of Fig. 14. (a) The magnet's presence causes a collective displacement of electrons in the $-y$ direction, resulting in a surface charge on the upper side of the superconductor having the same sign as that of the lower side of the magnet, leading to a repulsive interaction between them. (b) The breaking of symmetry occurs owing to the collective displacement of electrons in the y direction. As a result, the surface charge on the upper side of the superconductor is of the opposite sign compared to that of the lower side of the magnet, leading to an attractive interaction between them.

Meissner effect [28]. It is conventionally believed that superconductors placed in a weak external magnetic field $\mathbf{H}$ will expel the magnetic field from their interior upon cooling to below their transition temperature. Notably, the schematic diagram and explanation commonly used in textbooks and papers may not offer a comprehensive understanding of the experimental facts, leading to potential misunderstandings.

The magnetic field expelled picture of Fig. 13 shows that the Meissner effect is a time-dependent dynamic process. Hence, any valuable theory of superconductivity must be able to explain how the superconductor goes from the normal to the superconducting state by expelling the magnetic field against Faraday's law. Almost ninety years have passed since the first experiment conducted by Meissner and Ochsenfeld [28], and many theories and mechanisms have been proposed to explain the Meissner effect. However, as argued by Hirsch [25], these mechanisms fail to consistently describe the Meissner experiment. In this study, we aim to solve this puzzle by only employing the microscopic mechanism of proton-electron electric dipole pairing.

Before beginning the investigation, it is essential to examine the Meissner effect experiment [37]. Figure 14 includes two experiment screenshots that clearly demonstrate both repulsion and attraction between the superconductor and the magnet, as shown in Fig. 14 (a) and (b), respectively. Furthermore, repulsion or attraction can switch rapidly, indicating that the widely accepted mechanism of magnetic field expulsion shown in Fig. 13 (b) cannot explain why the superconductor and magnet of Fig. 14(b) attract each other. To better explain the Meissner effect, we conducted a force analysis on the magnetic suspension in Fig. 14 (a) and the superconductor suspension in Fig. 14 (b). Assuming the masses of the magnet and the superconductor are m and M, respectively, the repulsive force F_R and the attractive force F_A can be expressed as follows:

$$F_R = mg; \quad F_A = Mg, \tag{14}$$

where g is the acceleration of gravity.

The force balancing condition mentioned in Eq. (14) above may seem simple, but it contains important information about the Meissner effect. First, the Meissner effect is directional, and the direction of the force is automatically adjusted based on the movement trend, enabling the magnet and the superconductor to either attract or repel each other. Second, as suggested by Eq. (14), the Meissner effect can automatically adjust its strength to balance gravity according to the mass of the magnet or superconductor. This experimental result poses a major challenge for theoretical superconductivity researchers as stable levitation requires a steady external energy input from the point of view of energy conservation. In the Meissner effect experiment depicted in Fig. 14, the magnetic field is the only external factor present outside the superconductor, meaning it is also the sole source of the force responsible for the levitation phenomenon.

In order to test the reliability and consistency of our theory as a new mechanism of superconductivity, we must subject it to strict experimentation using the results from Fig. 14. As illustrated in Figure 15, when there is no external magnetic field and the temperature is below the critical temperature for superconductivity, the superconductor enters a Mott insulating state, and all the valence electrons will occupy the position of zero potential energy, indicated by the white circle in the figure. When a magnet ($\mathbf{H}_{\rm ext}$) is placed above a superconductor, as shown in Fig. 15 (a), the magnet tends to fall due to the gravitational field, increasing the strength of the magnetic field within the superconductor. This causes the electrons to move from their equilibrium positions, generating an induced

magnetic field ($\mathbf{H}_{\rm ind}$) in the opposite direction and a repulsive interaction between the magnet and the superconductor. Therefore, in the experiment depicted in Fig. 14(a), we can observe the magnet levitating after being repelled by the superconductor. As illustrated in Fig. 15(b), when the magnet is lifted away from the vicinity of the superconducting surface, gravity tries to separate the magnet and the superconductor, causing a decrease in magnetic field strength within the superconductor. To resist this, the electrons within the superconductor move upwards from their original positions, simultaneously exciting an induced magnetic field ($\mathbf{H}_{\rm ind}$) in the same direction as $\mathbf{H}_{\rm ext}$. Since the net charges on the nearest neighboring surfaces of the magnet and superconductor are of different signs, mutual attraction naturally occurs between them.

From our explanation above, the nature of the Meissner effect is not mysterious. It is merely a simple magnetic interaction between a magnetized superconductor and a magnet. They follow the fundamental principle of "two identical poles repel and two opposite poles attract." Is there repulsion or attraction between magnet and superconductor? It depends entirely on whether the electrons in the equilibrium position are downward or upward. Furthermore, according to Eq. (14), why is the levitation force (F_R or F_A) automatically adjustable? This question is related to the London penetration depth and will discuss in the next section.

Before concluding this section, we would like to discuss persistent current in superconducting rings briefly. The scientific community generally agrees that experiments have repeatedly confirmed the existence of a current that persists indefinitely in a superconducting circular loop. Some researchers have even estimated that the current in the ring could take up to 100 billion years to dissipate completely. However, this is purely a work of science fiction. Basic electromagnetic knowledge tells us that even in a vacuum and at absolute zero temperature, electrons moving in a circle will eventually lose their energy. The new theory presented in this paper challenges the notion of a superconducting current in a superconducting ring. According to this theory, the magnetic field measured in the experiment results from the magnetic field generated by the electron-proton electric dipoles present in the superconducting ring. In other words, the superconducting ring can be seen as a low-temperature magnet induced by the Meissner magnetization effect.

VII. LONDON PENETRATION DEPTH AND LEVITATION

The strength of the Meissner effect is usually described in terms of λ_L, which is according to the following formula [38]:

$$\mathbf{H}(x) = \mathbf{H}_0 e^{-x/\lambda_L}, \tag{15}$$

where $\mathbf{H}_0$ is a weak external magnetic field, $\mathbf{H}(x)$ is the decaying magnetic field inside the superconductor. The London penetration depth is given by

$$\lambda_L = \sqrt{\frac{mc^2\varepsilon_0}{n_s e^2}}, \tag{16}$$

where n_s is the density of superconducting electrons.

It is important to note that the theoretical values predicted by Eq. (16) do not align with experimental results. Numerous experiments have demonstrated that the penetration depth is closely linked to external magnetic field strength [68] and temperature [69, 70] and the shape, size, and orientation of superconducting samples. However, Eq. (16) fails to provide an internal correlation between penetration depth, temperature, and magnetic field. Essentially, London's theory is merely phenomenological and does not provide a dynamic explanation of how magnetic fields enter and expel the superconductor, let alone clarify the competition mechanisms among temperature, magnetic field, and penetration depth. As our present proton-electron electric dipole superconductivity theory is microscopic, it may enable us to study the dynamic processes of London's penetration depth.

A. Effective penetration depth

As our theory is based on the Mott insulator model rather than the Drude model, the density of superconducting electrons (n_s) does not exist within our framework. However, under our theoretical framework, one can define the electron density (n) as $1/\Omega$, where Ω represents the volume of a primitive unit cell of the studied superconductor. Moving forward, we will provide a qualitative explanation of the formation mechanism of penetration depth and identify the phys-

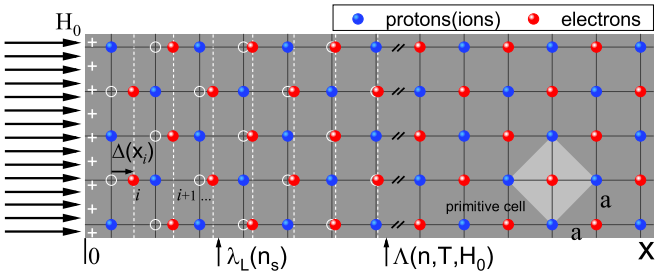

Figure 16: Microscopic explanation of London penetration depth: When a magnetic field $\mathbf{H}_0$ enters a superconductor along the x direction, the electromagnetic force causes the electrons near the surface of the superconductor to move from their ground state positions of zero potential (indicated by the white hollow circles on the left side of the figure) to higher potential excited states (represented by the solid red circles on the left side of the figure). As the distance x from the surface increases, the magnetic field energy absorbed by the electrons decays rapidly, and the displacement parameter $\Delta(x_i)$ decreases accordingly. When $x > \Lambda(n, T, H_0)$, then $\Delta(x_i) = 0$, and all the absorbed magnetic field energy disappears completely. As a result, the superconductor on the right side remains in the Mott insulating state.

ical quantities related to it from the energy conservation and transformation perspective.

For ease of discussion, we will continue to adopt the two-dimensional model illustrated in Fig. 16. When an external magnetic field is applied along the x-axis and enters the superconductor, it will interact with the electrons initially trapped at zero potential energy positions (indicated by the white hollow circles in the figure). These electrons become excited and gain magnetic field energy, causing them to deviate from their equilibrium positions along the direction of the magnetic field. The i-th array of electrons' displacement $\Delta(x_i)$ is directly proportional to the magnetic field energy acquired by the electrons. Notably, the magnetic field energy is converted into the potential energy of the electrons rather than being expelled from the superconductor through the development of a so-called Meissner surface current, as more commonly imagined. Additionally, it is evident from this figure that the London penetration depth $\lambda_L(n_s)$ falls short of reality. To better and comprehensively characterize the interaction process between the magnetic field and superconductor, this paper introduces the effective penetration depth (EPD) $\Lambda(n, T, H_0)$.

B. Quantized steps

Within our theory, the electrons inside a superconductor are localized and form crystal structures. Therefore, the magnetic field entering the superconductor is not continuously absorbed but instead absorbed periodically. As depicted in Fig.17, the magnetic field inside the superconductor does not decay continuously, as described by Eq. (15). Instead, it reveals a ladder structure (quantized steps) with increasing x. The step width in the figure represents the distance between electron columns (or, for 3D superconductors, the distance between electron layers). The step height represents the attenuation of magnetic field intensity resulting from the absorption of electrons, which is proportional to the number of electrons contained in the corresponding column or layer. Figs. 17(a) and (b) illustrate the relationship between the effective penetration depth and electron density. Suppose $a_2 < a_1$, in which case the corresponding electron density $n_2 > n_1$; the magnetic field energy will be absorbed faster in the latter case. Accordingly, $\Lambda(n_2, T, H_0) < \Lambda(n_1, T, H_0)$. For three-dimensional superconducting bulk materials, various external factors, such as magnetic field strength, temperature, material size and shape, crystal defects, crystal orientation, and so on, can influence the width and height of the steps in the figure, thereby potentially affecting the EPD.

We propose that the characteristics of a ladder-like structure in physical phenomena stem from the localization of electrons and that the structure's steps reflect the electrons' periodicity. In certain materials, particularly those that are two-dimensional or quasi-two-dimensional and subjected to extremely low temperatures and weak external fields, quantized steps are observable - examples include the quantum Hall effect [71, 72].

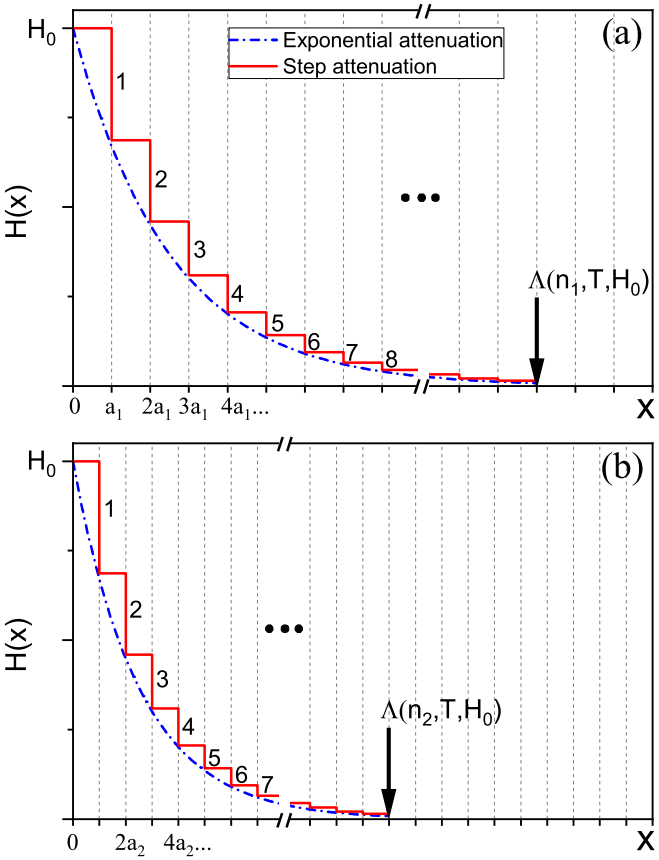

Figure 17: The new theory predicts a quantization step for penetration depth. (a) For low electron densities, larger penetration depths are observed. (b) As the electron density increases, the penetration depth decreases.

C. Superconducting magnetic levitation

As illustrated in Fig. 14, the EPD primarily regulates the net charge density near the superconductor's surface where the magnetic field enters. The surface layer of the superconductor exhibits a higher net charge density as the penetration depth increases. The net charge is zero without a penetration depth due to the balanced presence of positive and negative charges. In the magnetic levitation experiment depicted in Fig. 14, the magnet generates a non-uniform magnetic field whose strength varies with the distance and direction between the magnet and the superconductor. Consequently, the microscopic penetration depth can be controlled by manipulating the relative position between the macroscopic magnet and the superconductor. This, in turn, alters the net charge density on the superconductor's surface, ultimately resulting in the automatic dynamic balancing of the interaction between the magnet and the superconductor.

To explain the suspension experiment in Fig. 14(a) more intuitively, we will use the classical spring model to analyze how the superconductor automatically balances the force according to the weight of the magnet. Figure 18(a) shows a

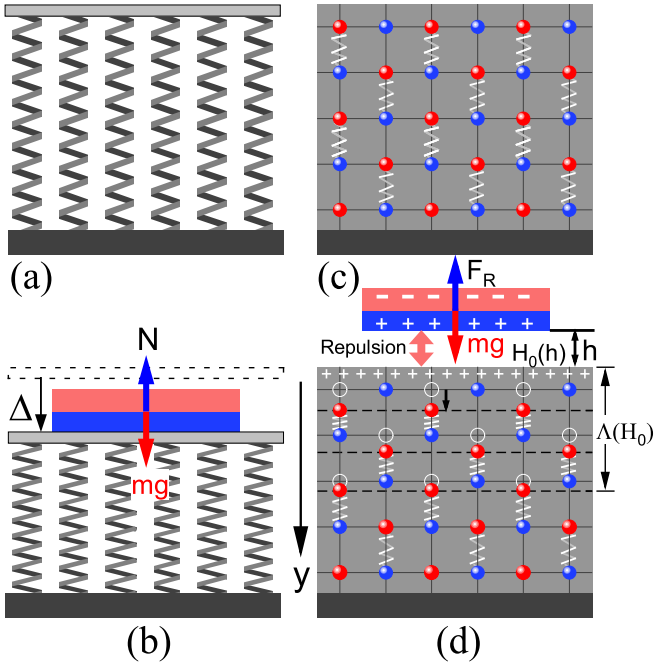

Figure 18: An analogy of superconducting levitation to a classical spring system. (a) A free spring system (assuming the mass of the spring is negligible); (b) an object m attains force balance by compressing the spring; (c) an insulating superconductor represented by "spring oscillators"; and (d) similar to the classical spring system in figure (b), the magnet is suspended by compressing the "springs" with the aid of the magnetic field.

set of springs in a free state. As shown in Fig. 18(b), when an object of mass m is placed on the springs, a reaction force N is caused by the compression spring (a proper deformation Δ) to achieve force balance $N = k\Delta = mg$ (where k is the spring coefficient).

Without an external magnetic field, a superconductor in an insulating state can be modeled as a spring oscillator, as shown in Fig. 18(c). Note that the lateral spring oscillators have been omitted from the figure. When a magnet with mass m is placed on top of the superconductor, the magnetic field causes the "spring oscillators" to compress and generate a combined reaction force F_R, as depicted in Fig. 18(d). The repulsive force F_R is proportional to the effective penetration depth $\Lambda(H_0)$, where H_0 denotes the magnetic field intensity of the magnet before entering the superconductor. Additionally, H_0 is a function of the distance h between the superconductor and the magnet, with smaller values of h leading to more significant values of H_0. Thus, the force balance $F_R = mg$ in Fig. 18(d) can be achieved by automatically adjusting the distance h based on the mass of the magnet. However, suppose the mass of the magnet is too heavy, and the electrostatic potential difference (EPD) exceeds its limit. In that case, the superconductor undergoes a phase transition from the magnetic state to the normal state, and the levitation effect is no longer sustainable.

Strictly speaking, the Meissner effect and the London penetration depth are not superconducting phenomena. They are just the low-temperature magnetization effects. By increasing the strength of the external magnetic field, which is equivalent to increasing the temperature, the electrons will gain more magnetic field energy and generate a more significant displacement. When the applied magnetic field is greater than the critical magnetic field $\mathbf{H}_c$ which functions as the Curie temperature of the superconductor, the magnetic state of the Meissner effect will be entirely or partially destroyed to the normal state of Fig. 10(b) for the type-I and type-II superconductors, respectively. In the next section, we will focus on the vortex state of the type-II superconductor.

VIII. PHYSICAL ORIGIN OF VORTEX LATTICES

Abrikosov proposed the concept of the vortex lattice in type-II superconductors in his pioneering work [42]. Since then, considerable theoretical and experimental efforts have been devoted to understanding its behavior [44–50]. However, to date, the mechanism behind it remains to be seen at the macroscopic level. The most fundamental question of how the magnetic field leads to the formation of vortex lattices is still challenging. What is the physical origin of the vortex state? Our theory provides new insights into the mechanisms behind vortex formation and why it disappears, which is no longer a puzzle.

A. Vortex state with coexistence of three phases

As depicted and explained in Fig. 19, when a superconductor is cooled below its critical temperature while an external magnetic field $\mathbf{H}$ is applied, it undergoes a series of phase transitions. Depending on the strength of the applied magnetic field, the superconductor can transition from an insulating state to a magnetic state, from a magnetic state to a normal state, or directly from an insulating state to a normal state. When the magnetic field satisfies $\mathbf{H}_{c1} < \mathbf{H} < \mathbf{H}_{c2}$, a vortex state with a mixture of insulating, magnetic, and normal regions is formed.

When the applied magnetic field strength $\mathbf{H}$ is zero, the superconductor is in the Mott insulating state depicted in Fig. 10(a). As the magnetic field strength increases, the superconductor undergoes a three-step phase transition. In the first step, which is also known as the Meissner transition and occurs when $\mathbf{H} < \mathbf{H}_{c1}$, the magnetic field energy absorbed by the electrons breaks the symmetry of the proton-electron electric dipole vector. This results in a phase transition from the insulating state of Fig. 10(a) to the magnetic state of Fig. 10(e) or (f) near the superconductor's surface within the EPD Λ. In the second step, which occurs when $\mathbf{H}_{c1} < \mathbf{H} < \mathbf{H}_{c2}$, the magnetic field strength continues to increase, leading to more tremendous energy and positional perturbations of the electrons. This disrupts the proton-electron electric dipole orientation order in some tubes, causing the magnetic state to

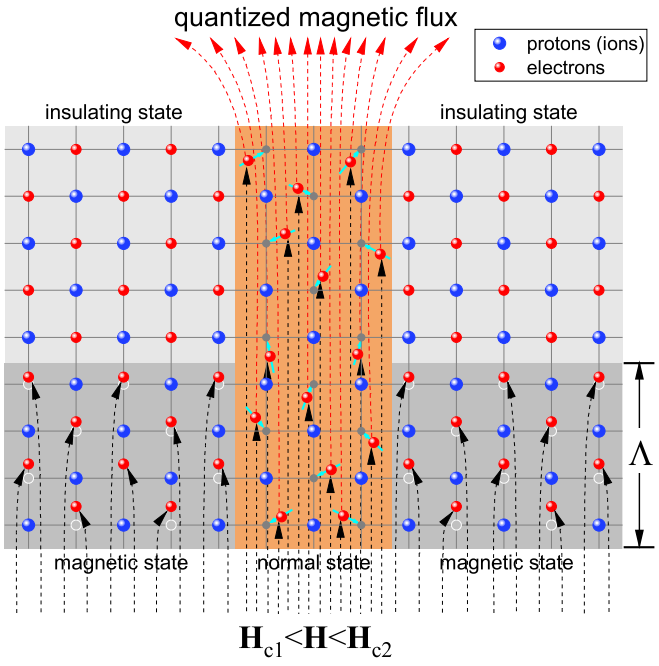

Figure 19: The microstructure of the vortex state in type-II superconductors exhibits the coexistence of three states. In the light gray region, electrons do not absorb the energy of the magnetic field and maintain the ground state of the Mott insulator. In the gray region, electrons absorb a small amount of energy and then undergo a Peierls phase transition to the Meissner magnetic state. Finally, in the orange region of normal state, the orientation order is completely disrupted as the electrons absorb enough energy.

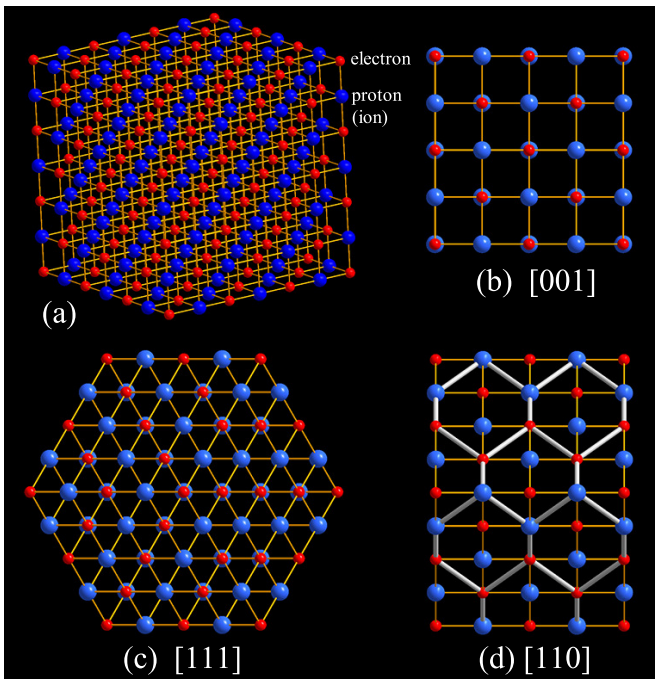

Figure 20: The 3D Mott insulator can be seen as the DNA of the vortex lattice. (a) A duplex lattice of proton(ion)-electron pairs with space-group $Fm\bar{3}m$; (b) the 2 × 2 super-cells of the crystal along the fourfold [001] direction; (c) the threefold [111] direction; and (d) the twofold [110] direction, respectively. For case (d), the rectangle lattice (the thin yellow bonds) can be rearranged as a distorted hexagonal lattice (the thick light gray bonds).

normal state and insulating state to normal state phase transitions to occur within the EPD region and inside the superconductor, respectively. It is important to note that the external magnetic field itself is not quantized inside the tubes. Instead, the quantized proton-electron electric dipole absorbs the magnetic field energy and emits a magnetic flux quantum $\Phi_0 = \mathrm{h}/2\mathrm{e}$. Finally, in the third step, when $\mathbf{H} > \mathbf{H}_{c2}$, all electrons have gained enough magnetic field energy to destroy the orientation order of the electric dipole (or magnetic vector), and the superconductor becomes a normal metal.

According to our theory, the phase transitions observed in the superconductor are fundamentally driven by the energy exchange between the magnetic field and the electrons of proton-electron electric dipoles. The occurrence of these phase transitions requires a contribution of magnetic field energy, and the maintenance of the new phase transition state requires a continuous energy supply from the magnetic field. Our research indicates that the proton-electron electric dipole inside the superconductor absorbs the external magnetic field. This explanation differs from the conventional picture, in which the magnetic field is either expelled or penetrates the superconductor in the form of vortices. Furthermore, as shown in the tubes depicted in Fig. 19, the experimentally observed quantized flux does not originate from the external magnetic field but rather from the local quantized proton-electron pair in the tube.

B. The DNA of vortex lattice

Numerous experimental results have been reported on the vortex lattice structures s [44–46], leading to two important conclusions. First, despite the wide range of classes and structures of superconductors, their vortex lattice structures exhibit very similar symmetries. Second, the vortex symmetry is closely related to the orientation of the applied magnetic field. Specifically, square, triangular, or distorted hexagonal vortex lattices can be observed when the field is applied along the fourfold (the [001] direction), threefold (the [111] direction), or twofold (the [110] direction) symmetric axis of the superconductor, respectively. To the best of our knowledge, such lattice symmetry precisely matches that of a $NaCl$-type lattice, as shown in Fig. 20 of a proton (ion)-electron lattice and its symmetry. This figure can be regarded as the "DNA" of the superconducting material, which determines the structure and symmetry of the vortex lattice.

It is clear that the perfect macroscopic symmetry observed in the vortex lattice originates from the intrinsic microscopic perfect symmetry of the proton (ion)-electron lattice, which can be considered the lattice's DNA, as illustrated in Fig. 21. The formation of the vortex structure still follows the princi-

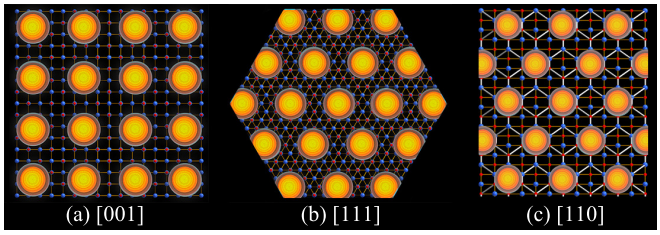

Figure 21: Matching relationship between three typical Abrikosov vortex lattices and the corresponding proton-electron electric dipole lattices. (a) A square vortex lattice in [001] direction; (b) a triangular vortex lattice in [111] direction; and (c) a distorted hexagonal vortex lattice in [110] direction.

ple of minimum free energy. When the symmetry of the vortex lattice matches that of the parent lattice of proton-electron pairs, the system's minimum free energy and the stability of the vortex lattice can be ensured. As the magnetic field strength increases, electrons absorb more magnetic field energy and move further away from their equilibrium positions, leading to a stronger interaction between proton-electron electric dipoles. This interaction disrupts the orientation order of more electric dipoles, which is manifested by an increase in the diameter and number of flux vortices observed experimentally. The orientation order of the electric dipoles is completely destroyed when the upper critical field is reached and the superconductor enters the normal state.

C. Vortex dynamics

Vortex dynamics is one of the most challenging problems in understanding type-II superconductors [50]. The magnetic flux vortex can form various states inside the superconductor [52], such as solid, liquid, and glass [73]. Experiments show that the magnetic flux vortex can have various forms of movement, such as hopping, creeping, and flowing. In the traditional theoretical framework, studying the movement of a vortex line requires knowledge of the external forces acting on the vortex line, such as driving force, friction force, collision force, pinning force, and Magnus force. This is a highly complex problem; no analytical or numerical solution is available. We wish to point out that the difficulty of this research also arises from the limitations of Drude's model. The conventional theory of vortex motion is based on the model of the random motion of carriers (electrons) in superconductors, which may not be accurate.

The formation of vortex lattices in superconductors requires two critical external conditions: first, sufficiently low temperature, and second, appropriate magnetic field strength. When the temperature and external magnetic field are low, magnetic flux lines distribute uniformly inside the superconductor and freeze to form an ordered lattice, as depicted in Fig. 21. In a type-II superconductor in the vortex state, the vortex and the surrounding non-vortex regions are distinct. What is

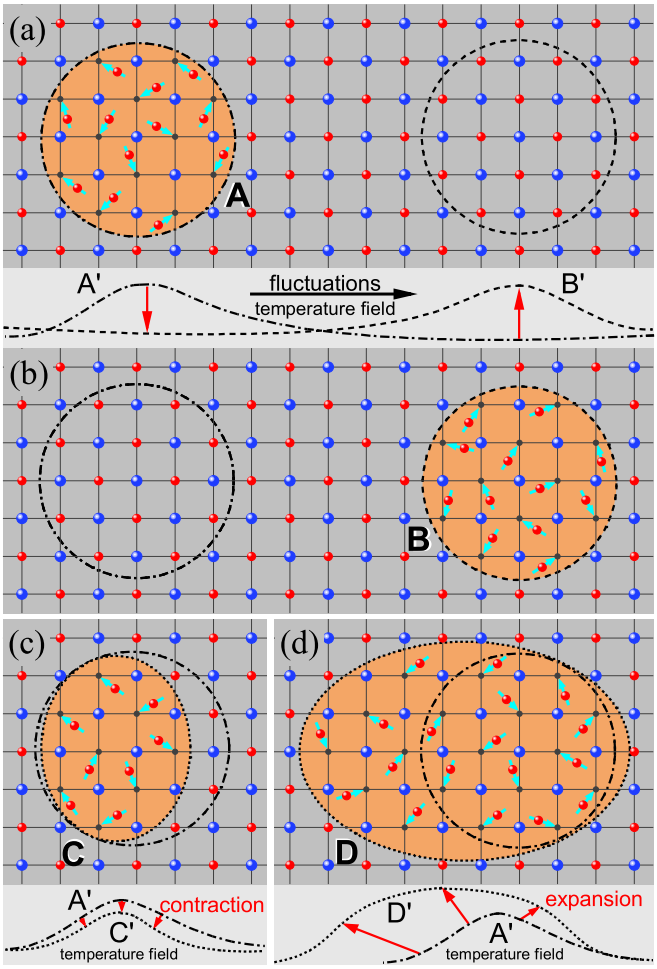

Figure 22: Top view of vortex hopping and creeping, a simple graphical explanation of vortex motion in type-II superconductors. (a) A vortex is formed in the region **A** due to the existence of the temperature field peak A' around the region, see the dot-dash line in the figure below; (b) thermal fluctuations lead to the annihilation of the temperature peak A' and corresponding vortex in region **A**, and at the same time generate new temperature peak B' and corresponding vortex in region **B**, as shown the dashed line in the figure. This process is misinterpreted as the movement (hopping) of the same vortex from **A** to **B**; (c) and (d) the vortex **A** can contract to **C** or expand to **D** in situ based on thermal fluctuations (A' to C', or A' to D'), often interpreted as creeping vortex dynamics.

the fundamental physical difference between the vortex and non-vortex regions? The proton-electron pairing mechanism proposed in this paper suggests that the electrons of proton-electron electric dipoles inside the vortex region absorb more magnetic field energy and gain higher free energy, leading to a higher temperature in the inner vortex than the outer vortex. This conclusion implies that magnetic field or temperature instability can trigger a change in the vortex region, which is the fundamental physical reason for the instability and motion of the vortex lattice in the superconductor.

In the following, we will explain the phenomena of vortex

hopping, flowing, and creeping using Fig. 22. Fig. 22(a) shows an initial vortex element of area $\mathbf{A}$. Consequently, there is a temperature field peak A' around the vortex's core, as shown by the dot-dash line in the figure. As the temperature or magnetic field increases, the uniformity of the temperature and magnetic field inside the superconductor will decrease, resulting in large random fluctuations in temperature and magnetic field. Due to random fluctuations in temperature, the peak A' of the temperature field around vortex $\mathbf{A}$ may suddenly disappear. All the electrons inside the vortex return to equilibrium, causing the vortex to disappear as well. As shown in Fig. 22(b), almost simultaneously with the disappearance of peak A', a temperature peak B' may suddenly appear in the nearby region $\mathbf{B}$ (the dashed line in the figure). The higher temperature intensifies the thermal vibrations of the electrons in the region, causing them to leave their original equilibrium positions and exciting a new vortex $\mathbf{B}$ as shown on the right of Fig. 22(b). During this process, the vortex seems to move (or jump) from $\mathbf{A}$ to $\mathbf{B}$. Temperature fluctuations may also occur in situ, as illustrated by the dot lines C' in Fig. 22(c) and D' in Fig. 22(d) below. In this case, the vortex $\mathbf{A}$ may sometimes shrink into a thin vortex $\mathbf{C}$ of Fig. 22(c) or expand into a fat vortex $\mathbf{D}$ of Fig. 22(d), which is experimentally observed as vortex creeping.

According to our theoretical framework, the movement (or change) occurs in the temperature and magnetic fields rather than in the carriers (electrons) within the vortex core, as previously thought. Vortices are generated and annihilated through a fundamental physical process by changing the external magnetic field and temperature. Microscopically, this process changes the orientation of the proton-electron electric dipole (magnetic vector) due to temperature and magnetic field instability. Notably, our new theory eliminates the need for the so-called flux pinning mechanism, previously used to prevent "flux creep" in superconductors. With the proton-electron pairing mechanism, the flux vortices are naturally confined and localized within the superconductor.

IX. CONCLUDING REMARKS

This paper has achieved two fundamental unification by utilizing three well-known scientific hypotheses: the Mott insulator, Maxwell's displacement current, and the Dirac magnetic monopole. Firstly, the unification of particles, where the hydrogen atom, neutron, electric dipole, capacitor, and magnetic monopole are all electron-proton pairs. Secondly, the unification of fields and concepts, where the magnetic field, magnetic moment, spin, magnetic dipole field, displacement current, and order parameter are all electric fields generated by electron-proton pairs. We establish a unified theory of electron-proton local pairing in real space, which is different from the BCS theory of electron-electron non-local pairing in k-space. The pairing mechanism in the new theory is based on the principle of ?opposites attract,? eliminating the need to introduce any quasi-particle pairing glue. The superconducting phenomenon in this theory arises from the most direct Ginzburg-Landau symmetry-breaking phase transition caused by Peierls transitions, which can be reached through a small collective displacement of valence electrons from their equilibrium positions when an appropriate temperature and external field are applied. Surprisingly, while combining Maxwell's theory with Dirac's magnetic monopole theory, we have successfully realized a perfect mathematical symmetry in Maxwell's equations and unified electromagnetic properties.

To test the proton-electron pairing mechanism, we have proposed that the proton-electron electric dipole vector serves as the order parameter of the Ginzburg-Landau theory of superconducting phase transitions. In this theoretical framework, the dynamic interaction between the proton-electron electric dipole and the external magnetic field has well explained several crucial superconducting phenomena, including the Meissner effect, the London penetration depth, the vortex lattices, and the vortex dynamics. Notably, even below the superconducting transition temperature, a superconductor may exist in one of five distinct states: insulating, normal, metallic, magnetic, or superconductive. The Meissner effect, which denotes the coexistence of insulating and magnetic states, and the vortex state, denoting the coexistence of insulating, magnetic, and normal states, further highlight the importance of understanding these states. Additionally, the proton-electron electric dipoles can self-organize into electric dipole crystals (3D Mott insulator) with space-group $Fm\bar{3}m$ through electromagnetic interaction, which serves as the microscopic foundation of the vortex lattices of type-II superconductors.

We recognize that the field of theoretical physics has been stagnant for decades. To make progress, physics requires innovative and unconventional ideas that challenge established theories and models which are no longer adequate due to modern experiments. We propose that the proton-electron pairing mechanism may provide new insights into all physical problems. In cuprate superconductors with high-temperature, there is controversy regarding the origin of phenomena such as the pseudogap [74, 75], charge stripes [64, 65], checkerboard phases [39], electron nematic phase [76], magic doping [40, 41], charge density waves (CDW) [77], etc. These disputes are still hotly debated in the condensed matter community. Our theoretical framework can definitely resolve these debates. Studies show that they are related to the symmetry of the proton-electron electric dipole. In addition, the proton-electron pair is responsible for the quantum Hall effect [71, 72] and the Hall anomaly [78, 79] in superconductors. More detailed explanations of these findings will be presented in another article.

Before concluding this article, it is essential to raise a critical question: why do identical proton-electron pairs, such as neutrons and hydrogen atoms, display notably different physical properties? This query represents a fundamental yet unresolved enigma in physics because it deals with the nature of the vacuum. As a reasonable assumption, there must be a

fitting external binding energy to link protons and electrons, forming a stable composite particle. We believe this contribution originates solely from the vacuum. These binding energies can be entirely or partially released depending on specific circumstances, leading to characteristic spectra for hydrogen atoms and neutrinos for neutrons. We consider photons and neutrinos to be quasiparticle modes of vacuum energy. The community of physicists should agree that the vacuum is not empty, as it holds infinite energy.

The author would like to acknowledge Prof. Duan Feng for his invaluable suggestions and helpful discussions at the early stage of this research. Special thanks go to Prof. Dingyu Xing for his supportive and considerate care of the author's personal and family life. The author would also like to express his appreciation to Prof. Changde Gong for giving him the opportunity to comprehend the fascinating world of superconductivity. Finally, the author extends his deepest gratitude to Prof. Shusheng Jiang for his unwavering encouragement, support of the research process, and provision of both living arrangements and research resources, which served as the driving force and determination necessary to overcome scientific challenges.

* Electronic address: xiuqing_huang@163.com

[1] H. K. Onnes, Leiden Comm. **119b**, 122 (1911).
[2] H. G. Smith and J. O. Wilhelm, Rev. Mod. Phys. **7**, 237 (1935).
[3] J. Eisenstein, Rev. Mod. Phys. **26**, 277 (1954).
[4] J. G. Bednorz and K. A. Muller, Z. Phys. B. **64**, 189 (1986).
[5] M. K. Wu, et al., Phys. Rev. Lett. **58**, 908 (1987).
[6] M. A. Subramanian, et al., Science **239**, 1015 (1988).
[7] A. W. Sleight, Science **242**, 1519 (1988).
[8] A. W. Sleight, J. L. Gillson, and P. E. Bierstedt, Solid State Communications **88**, 841 (1993).
[9] J. Nagamatsu, et al., Nature. **410**, 63 (2001).
[10] Y. Kamihara et al., J. Am. Chem. Soc. **130**, 3296 (2008).
[11] A. P. Drozdov et al., Nature **525**, 73 (2015).
[12] J. Bardeen, L. N. Cooper and J. R. Schrieffer, Phys. Rev. **106**, 162 (1957).
[13] P. W. Anderson, Science **235**, 1196 (1987).
[14] G. Baskaran and P. W. Anderson, Phys. Rev. B **37**, 580(R) (1988).
[15] J. R. Schrieffer, X. G. Wen, and S. C. Zhang Phys. Rev. Lett. **60**, 944 (1988).
[16] P. Monthoux, A. V. Balatsky, and D. Pines, Phys. Rev. Lett. **67**, 3448 (1991).
[17] E. Dagotto, Rev. Mod. Phys. **66**, 763 (1994).
[18] D. J. Van Harlingen, Rev. Mod. Phys. **67**, 515 (1995).
[19] E. Demler and S. C. Zhang, Nature **396**, 733 (1998).
[20] E. Demler, W. Hanke, and S. C. Zhang, Rev. Mod. Phys. **76**, 909 (2004).
[21] Christoph J. Halboth and Walter Metzner Phys. Rev. Lett. **85**, 5162 (2000).
[22] P. A. Lee, N. Nagaosa and X. G. Wen, Rev. Mod. Phys. **78**, 17 (2006),
[23] Adam Mann, Nature **475**, 280 (2011).
[24] P. W. Anderson, Science **317**, 1705 (2007).
[25] J. E. Hirsch, Phys. Scr. **80**, 035702 (2009).
[26] J. E. Hirsch, Phys. Scr. **85**, 035704 (2012).
[27] J. E. Hirsch, M. B. Maple and F. Marsiglio, Physica C, **514**, 1 (2015).
[28] W. Meissner and R. Ochsenfeld, Naturwiss. **21**, 787 (1933).
[29] V. L. Ginzburg and L. D. Landau, Zh. Eksp. Teor. Fiz. **20**, 1064 (1950).
[30] N. F. Mott and R. E. Peierls, in Proc. Phys. Soc. **49**, 72 (1937).
[31] J. Orenstein, and A. J. Millis, Science **288**, 468 (2000).
[32] S. M. Hayden, et al., Nature **429**, 531 (2004).
[33] H. He, et al., Science **295**, 1045 (2002).
[34] Yawen Fang, et al., Nature Physics **18**, 558 (2022).
[35] J. C. Maxwell, Philos. Mag. J. Sci., London, Edinburg and Dubline, Fourth series, 161 (1861).
[36] P. A. M. Dirac, Proc. Roy. Soc. **A 133**, 60 (1931).
[37] https://www.reddit.com/r/gifs/comments/1q0d8n/the_meissner_effect/
[38] F. London and H. London, Proc.Roy.Soc. **A149**, 71 (1935).
[39] T. Hanaguri, et al., Nature, **430**, 1001 (2004).
[40] S. Komiya, H. D. Chen, S. C. Zhang, and Y. Ando, Phys. Rev. Lett. **94**, 207004 (2005).
[41] H. D. Chen, S Capponi, F. Alet, and S. C. Zhang Phys. Re. B **70**, 024516 (2004).
[42] A. A. Abrikosov, Zh. Eksp. Teor. Fiz. **32** , 1442 (1957).
[43] A. A. Abrikosov Rev. Mod. Phys. **76**, 975 (2004).
[44] U. Essmann, and H. Traeuble, Phys. Lett. **24A**, 526 (1967).
[45] P. L. Gammel, et al., Phys. Rev. Lett. **59**, 2592 (1987).
[46] H. F. Hess, et al., Phys. Rev. Lett. **62**, 214 (1989).
[47] G. Blatter, M. V. Feigel'man, V. B. Geshkenbein, A. I. Larkin, and V. M. Vinokur, Rev. Mod. Phys. **66**, 1125 (1994).
[48] K. Harada, O. Kamimura, H. Kasai, T. Matsuda, Science **274**, 1167 (1996).
[49] Q. Niu, P. Ao and D. J. Thoulesss, Phys. Rev. Lett. **72**, 1706 (1994).
[50] Y. Bugoslavsky, et al., Nature **410**, 63 (2001).
[51] H. Yang, et al., Nature Physics, **7**, 325 (2011).
[52] Mark W. Coffey and John R. Clem, Phys. Rev. Lett. **67**, 386 (1991).
[53] A. M. Campbell and J. E. Evetts, Advances in Physics **21**, 199 (2006).
[54] T. Nattermann and S. Scheidl, Advances in Physics **49**, 607 (2010).
[55] G. E. Uhlenbeck and S. Goudsmit, Nature, **117**, 264 (1926).
[56] P. Drude, Annalen der Physik **1**, 369 (1900).
[57] P. Drude, Annalen der Physik **1**, 566 (1900).
[58] A. Sommerfeld, Naturwiss. **15**, 825 (1927).
[59] M. Planck, Ann. Phys. **1**, 69 (1900).
[60] A. A. Michelson and E. W. Morley, American Journal of Science **34**, 427 (1887).
[61] W. Gerlach and O. Stern, Z. Phys. **9**, 349 (1922).
[62] J. E. Hirsch Phys. Rev. B **31**, 4403 (1985).
[63] C. Kim, et al., Phys. Rev. Lett. **77**, 4054 (1996).
[64] S. A. Kivelson, et al., Rev. Mod. Phys. **75**, 1201 (2003).
[65] Y. Jiang, et al., Nature **573**, 91 (2019).
[66] S. Raghu, A. Kapitulnik, and S. A. Kivelson Phys. Rev. Lett. **105**, 136401 (2010).
[67] K. Sengupta, et al., Phys. Rev. B **63**, 144531 (2001).
[68] A. Maeda, et al., Phys. Rev. Lett. **74**, 1202 (1995).
[69] D. H. Wu, et al., Phys. Rev. Lett. **70**, 85 (1993).
[70] F. Gross, Z. Phys. B, **64**, 175 (1986).
[71] Horst L. Stormer, Rev. Mod. Phys. **71**, 875 (1999).
[72] Yuanbo Zhang, Yan-Wen Tan, Horst L. Stormer, and Philip Kim, Nature **438**, 201 (2005).
[73] S. A. Kivelson, E. Fradkin and V. J. Emery, Nature, **393**, 550 (1998).

[74] Tom Timusk and Bryan Statt, Rep. Prog. Phys. **62**, 61 (1999).
[75] H. Ding, et al., Nature **382**, 51 (1996).
[76] M. J. Lawler, et al., Nature, **4**66, 347 (2010).
[77] G. Campi, et al., Nature, **525**, 359 (2015).
[78] S. J. Hagen, et al., Phys. Rev. **B 41**, 11630(R) (1990).
[79] Q. L. He, et al., Science **357**, 294 (2017).